THERMAL HYDRAULIC ANALYSIS OF MH-1A CORE 5

Henry C. Gignilliat, et al

Army Engineer Power Group
Fort Belvoir, Virginia

1 May 1974

UNCLASSIFIED
SECURITY CLASSIFICATION OF THIS PAGE (When Data Entered)

REPORT DOCUMENTATION PAGE		READ INSTRUCTIONS BEFORE COMPLETING FORM
1. REPORT NUMBER USAENPG-ED 7401	2. GOVT ACCESSION NO.	3. RECIPIENT'S CATALOG NUMBER
4. TITLE (and Subtitle) THERMAL HYDRAULIC ANALYSIS OF MH-1A CORE 5		5. TYPE OF REPORT & PERIOD COVERED Final Report 6. PERFORMING ORG. REPORT NUMBER NA
7. AUTHOR(s) Henry C. Gignilliat Thomas M. Rotchford Peter E. Francisco Randal M. DeVault		8. CONTRACT OR GRANT NUMBER(s) NA
9. PERFORMING ORGANIZATION NAME AND ADDRESS U.S. Army Engineer Power Group (USAENPG-ED) Fort Belvoir, VA 22060		10. PROGRAM ELEMENT, PROJECT, TASK AREA & WORK UNIT NUMBERS NA
11. CONTROLLING OFFICE NAME AND ADDRESS U.S. Army Engineer Power Group (USAENPG-ED) Fort Belvoir, VA 22060		12. REPORT DATE 1 May 1974 13. NUMBER OF PAGES 94
14. MONITORING AGENCY NAME & ADDRESS(if different from Controlling Office) NA		15. SECURITY CLASS. (of this report) UNCLASSIFIED 15a. DECLASSIFICATION/DOWNGRADING SCHEDULE NA

16. DISTRIBUTION STATEMENT (of this Report)

Approved for public release; distribution unlimited.

17. DISTRIBUTION STATEMENT (of the abstract entered in Block 20, if different from Report)

NA

18. SUPPLEMENTARY NOTES

NA

19. KEY WORDS (Continue on reverse side if necessary and identify by block number)

Nuclear reactor	Thermal analysis, reactor
Safety, nuclear	STURGIS
Fuel densification, nuclear	MH-1A reactor
Reactor transients	Reactor protection

20. ABSTRACT (Continue on reverse side if necessary and identify by block number)

This report presents steady-state and transient thermal analyses of the MH-1A Floating Nuclear Power Plant Core 5 for normal operation and anticipated transients. The reactor core safety limits, which form the basis for safe operation and core protection, are established in terms of measurable reactor parameters. The ability of the reactor protection system to prevent violation of the core safety limits is demonstrated. The steady-state analysis includes an evaluation of the fuel and cladding temperature distribution and the

DD FORM 1 JAN 73 1473 EDITION OF 1 NOV 65 IS OBSOLETE

UNCLASSIFIED
SECURITY CLASSIFICATION OF THIS PAGE (When Data Entered)

PRICES SUBJECT TO CHANGE

20. Continued

limiting heat flux and coolant enthalpy conditions. The report also presents analyses of limiting reactor transients including uncontrolled rod withdrawal in the power range and during source-level startup, secondary system steam-line rupture, and loss of reactor-coolant flow due to loss of power to both pumps. An addendum to the report presents an analysis and discussion of the effects of fuel densification on core performance.

THERMAL HYDRAULIC ANALYSIS OF MH-1A CORE 5

HENRY C. GIGNILLIAT
PETER E. FRANCISCO
THOMAS M. ROTCHFORD
RANDALL M. DEVAULT

1 May 1974

ENGINEERING DIVISION
U. S. ARMY ENGINEER POWER GROUP
CORPS OF ENGINEERS

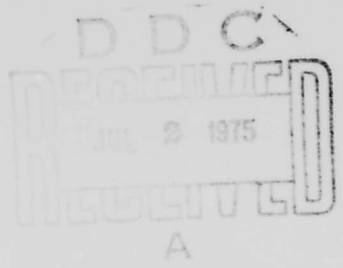

The findings of this report are not to be construed as an official Department of the Army position, unless so designated by other authorized documents.

THERMAL HYDRAULIC ANALYSIS OF MH-1A CORE 5

SUMMARY

This report presents the thermal hydraulic analysis of Core 5 for the MH-1A Floating Barge Nuclear Power Plant. The primary purpose of this study is to demonstrate that the reactor core is capable of meeting normal steady-state and transient performance requirements without violating the integrity of the fuel-element cladding. The analyses presented herein define the limits of safe operation for the core in terms of measurable reactor parameters: Reactor power, primary system pressure, coolant temperature and flow. The reactor protection system is designed to trip the reactor to protect the core in the event that reactor parameters approach the core design limits. The steady-state thermal analysis shows that the prescribed setpoints with allowance for error assure protection during all normal operations. The analysis of limiting reactor transients caused by operator error or equipment malfunction demonstrates the adequacy of the protection system in assuring that core limits are not exceeded during anticipated transient conditions.

TABLE OF CONTENTS

LIST OF TABLES

LIST OF FIGURES

LIST OF FIGURES (CONTINUED)

I. INTRODUCTION

A. Scope of Report

Section I gives a summary plant description, discusses the Type II fuel design, and presents the general thermal hydraulic parameters pertinent to the core analysis.

Section II is a safety evaluation summarizing the analyses that demonstrate the adequacy of the protection system during steady-state and transient conditions. The section includes a discussion of the normal plant operating limits and reactor core safety limits.

Section III defines the criteria that provide the basis for determining the core safety limits and for evaluating the reactor protection system.

Section IV contains a description of the steady-state core thermal analysis, which includes the evaluation of fuel and cladding temperature distribution, limiting heat flux, and coolant enthalpy conditions.

Section V presents the analysis of the limiting reactor transients. These transients include uncontrolled rod withdrawal in the power range and during source-level startup, secondary-system steam-line rupture, and loss of reactor coolant flow due to loss of power to both pumps.

B. Plant Description

The MH-1A Floating Nuclear Power Plant (STURGIS) is designed to serve the U.S. Army as a mobile source of power at any site accessible by waterways. The MH-1A can be utilized as a source of electrical power for a variety of missions. It is towed to a mooring site, secured, and put into service. The reactor is not operated during towing or associated transitory operations.

The nuclear power plant is installed in a floating mount consisting of a Liberty Ship hull, modified by the addition of a new midbody. All of the original propulsion equipment has been removed, and the nuclear reactor and associated equipment have been located in the new midbody. The design of the floating mount is in keeping with commercial marine standards consistent with the applicable rules and regulations of the U.S. Coast Guard and the American Bureau of Shipping. For added protection, a collision barrier and a deeper inner bottom are provided.

The electrical generating system is used to generate the electricity required for plant operation as well as the 10 MWe for shore distribution. Either 50- or 60-cycle alternating current can be supplied (the 50-cps operation allows a maximum net output of 8.05 MWe).

The heart of the nuclear system is a 45-MWt pressurized-water reactor. The nuclear core utilizes low-enriched pellets of uranium dioxide in tubular fuel elements, boron steel control rods with stainless steel followers, and a single-pass coolant flow.

The single reactor primary-coolant loop and all associated equipment are housed in a containment vessel. Two canned-rotor main coolant pumps mounted in parallel are required for reactor loop operation. The system pressurizer utilizes an electric heater and water quench system for maintaining proper pressure during operation. A vertical U-tube steam generator is used to supply steam to the main turbine.

The coolant enters the reactor vessel through a single inlet nozzle located in a plane above the core, flows down in flow paths between the vessel and core barrel, and makes a 180-degree upward turn. The coolant then passes through the lower orifice plate, which reduces any maldistribution caused by the inlet conditions, and through a lower grid plate, which distributes the flow to the fuel elements, control rods, and inner thermal shields. After passing through the core, the reactor exit plenum, and hot-leg piping, the primary coolant enters the steam generator, where heat is transferred from reactor coolant to the secondary water on the shell side, producing steam for the main turbine.

Fuel is contained within free-standing, fully-annealed, type 348 stainless steel tubing. Adequate radial pellet clearances are provided to assure pellet assembly and freedom for fuel swelling. A fission-gas plenum is provided in each fuel tube for the collection of released fission gases.

The core contains 12 cruciform-shaped control rods with stainless steel followers. The control-rod material is type 304 stainless steel, containing boron enriched in the isotope boron-10. The control material and followers are clad with type 348 stainless steel.

C. Type II Core Design

MH-1A Type II Core (reference 1)[1] consists of 32 fuel assemblies designed for full core (batch) loading and an increased core lifetime. The major changes in the Type II design affecting performance of the fuel consist of an increase in U-235 enrichment and the addition of burnable poison rods replacing certain fuel rods. These changes increase the burnup capability of the core while controlling reactivity and power distribution during core life.

The mechanical configuration of the fuel assembly is essentially unchanged from the Type I design, and therefore no changes in core average-flow characteristics are expected. However, the thermal performance of the fuel is affected by the reduced number of fuel rods in the core resulting from the insertion of burnable poison rods. This reduction in number of fuel rods increases the average power per rod (kw/ft) and the core average heat flux. However, improvements in the power distribution of the Type II core and additional operating restrictions placed on the plant result in a net reduction in peak power and heat flux from the previous Type I cores.

The nominal plant operating conditions are unchanged from the Type I cores and consist of the following:

---

[1] F. E. Muellner, et. al, "Type II Core Design for the MH-1A", NUS-576, Vols. 1 & 2, September 1970.

1. Core thermal power of 45 mw
2. Design coolant flow of 8650 gpm
3. System pressure of 1400 psia
4. Coolant inlet temperature of 476°F

The effect of fuel densification on the Type II fuel performance has been analyzed and is discussed in the addendum. The general thermal hydraulic characteristics of Core 5 are summarized in Table 1.

TABLE 1

THERMAL AND HYDRAULIC CHARACTERISTICS OF MH-1A CORE 5

Rated power level, MW	45
Btu/hr	1.53×10^8
Heat generated in the fuel, %	96.6
Pressure	
Nominal, psia	1400
Minimum steady-state, psia	1317
Coolant flow (nominal)	
Total flow, lb/hr	4.40×10^6
Coolant flow to inner thermal shields, %	2.3
Total coolant leakage flow, %	8.8
Effective core flow rate, lb/hr	4.01×10^6
Core flow area, ft^2	5.22
Average coolant mass velocity, lb/hr-ft^2	0.796×10^6
Average velocity along fuel rods, ft/sec	4.3
Coolant temperature	
Nominal inlet temperature, ^oF	476
Maximum inlet, steady-state, ^oF	492
Average rise in vessel, ^oF	30.3
Nominal outlet of vessel, ^oF	506.3
Nominal core bulk outlet temperature, ^oF	509
Heat transfer (at rated power)	
Active heat transfer area, ft^2	1204
Core average heat flux, Btu/hr-ft^2	0.123×10^6
Average linear heat rate of rod, kw/ft	4.8
Maximum linear heat rate, kw/ft	16.0(1)
Maximum UO_2 temperature, ^oF	4100
Average core enthalpy rise at rated power Btu/lb	38.2
Hot channel (115% overpower)	
Reactor power, MW_t	51.8
Maximum heat flux, Btu/hr-ft^2	0.529×10^6
Maximum UO_2 temperature ^oF	4400
Maximum clad surface temperature, ^oF	612
W-3 DNBR (minimum)	1.59

(1) Beginning of life equilibrium Xenon

II. SAFETY EVALUATION

This section discusses the selection of the safety system setpoints and the margins that these setpoints assure with respect to the safety limits. A summary of the protective systems settings for MH-1A Core 5 is presented, including the alarm setpoints and reactor trip setpoints and the effects of associated instrument error on each. Subsequent paragraphs discuss safety limits and summarize the conclusions of the steady-state and transient analyses.

A. Safety Limits

The basis for the determination of safety system setpoints is that given in AEC General Criterion 10 (Ref. 2)[1]:

> "Criterion 10 - Reactor design. The reactor core and associated coolant, control, and protection systems shall be designed with appropriate margin to assure that specified acceptable fuel design limits are not exceeded during any condition of normal operation, including the effects of anticipated operational occurrences."

The concept of a safety limit is further described in the "Guide on Content of Technical Specifications for Nuclear Reactors", also an AEC document.

> "The safety limit is a value of the chosen variable at which one can say with confidence that no serious consequences will occur. If the value of the variable were to be at this limit and all other variables at the upper bound of their operating range, and if all uncertainties in technical knowledge of the process were resolved unfavorably, no hazard to the public would exist."

The limiting safety system settings are established so as to assure that core damage will not occur during normal operation and anticipated transient conditions by preventing reactor parameters from approaching or exeeding the safety limits. The basis for determining the core safety limits is the protection of the fuel cladding - the first barrier to the unsafe release of fission products. The integrity of the fuel cladding is assured by (1) preventing fuel centerline temperatures from reaching to melting point under all operating conditions, and (2) preventing departure from nucleate boiling (DNB) or flow instability which can lead to DNB. The occurrence of DNB must be prevented because of the resultant large decrease in heat transfer capability of the cladding surface, and the possibility of cladding failure due to high temperature.

Safety limits have been developed for observed system parameters used in monitoring the behavior of the reactor plant. Figure 1 shows the reactor core safety limits for thermal power, coolant temperature, and pressure at the design flow rate of 8650 gpm. The area of safe normal operation is below these lines. A safety limit is considered to be exceeded if the point defined

---

[1] "General Design Criteria for Nuclear Power Plant Construction Permits", Proposed Amendment to 10CFR Part 50, Federal Register Vol 32, No. 132, July 11, 1967.

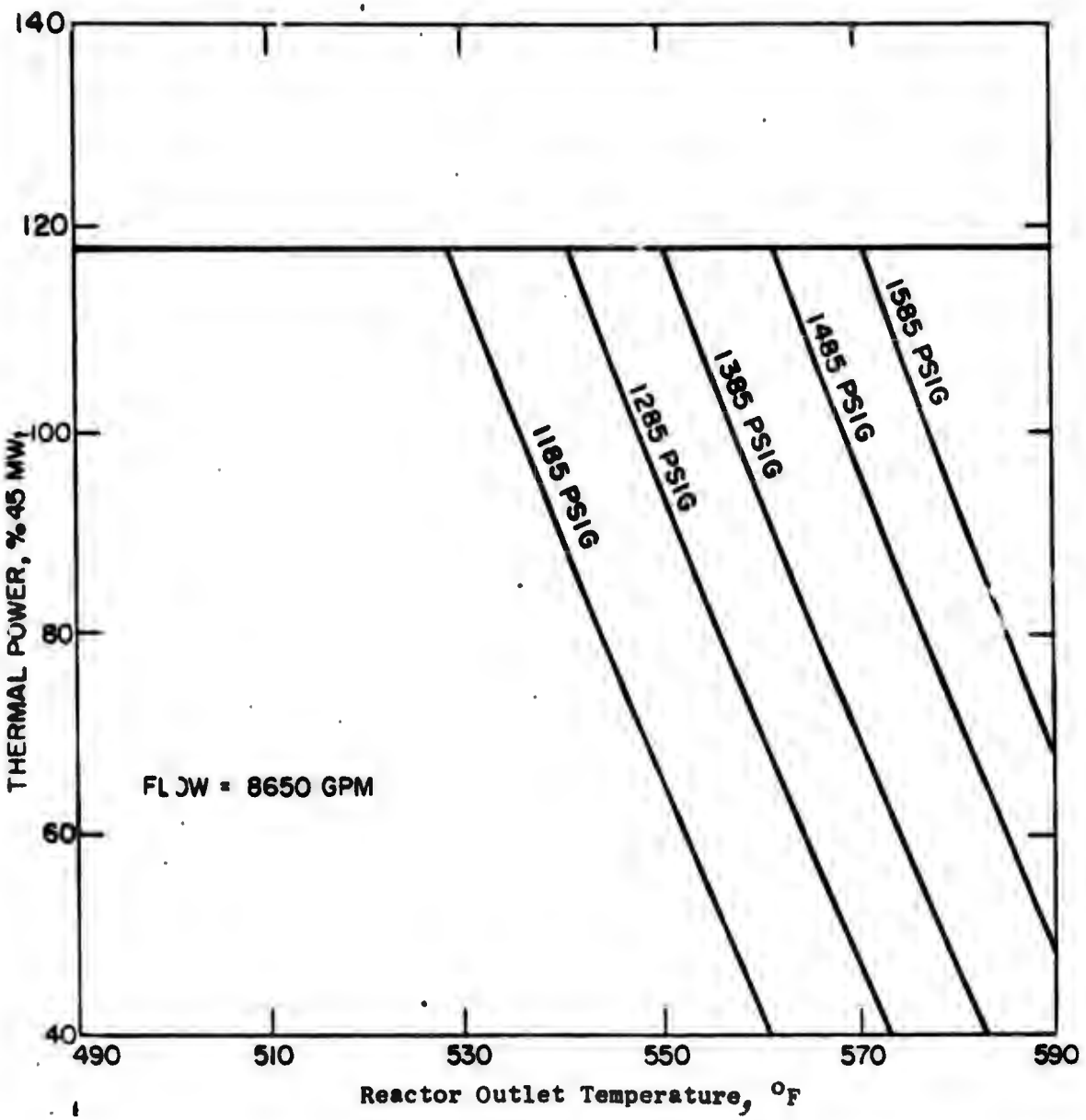

FIGURE 1 – REACTOR SAFETY LIMITS

by the combination of reactor outlet temperature and power level is at any time above or to the right of the appropriate limit corresponding system pressure. The pressure curves shown in Figure 1 represent the loci of points of reactor power and coolant temperature for which the minimum DNBR is no less than 1.30 and the maximum coolant void fraction is no greater than 0.32.

The safety limits represented by these curves should be interpreted properly as the maximum allowable rate of heat transfer from the fuel to the coolant (thermal power). Note that the rate of heat generation (neutron flux level) is equal to the rate of heat transfer to the water only if the neutron flux is not varying with time. In the case of power excursion, the rate of heat transfer to the coolant can exceed the safety limit only if the nuclear flux level remains in excess of it for a sufficient length of time. Analysis of specific transient conditions determines whether an actual safety limit has been violated.

It should be noted that these safety limit curves are not a basis for normal operation. Normal plant operations are well within the limits specified by these curves. For adverse operating conditions, the reactor protection system is designed to actuate a reactor trip before a safety limit is reached to assure that core design limits are not exceeded.

B. Normal Operating Limits

The normal operating band is defined by limits above and below the nominal full power value of each prime system variable. For the MH-1A, the prime system variables are reactor thermal power, primary system pressure, reactor coolant temperature, and flow. Determination of the operating band is based on observed deviations during normal plant transients (i.e., load changes), on permitted deviations during steady-state operation, and on control system deadband and overshoot.

Instrumentation, including visual and audible alarms, is provided for monitoring reactor parameters. In the event of deviations from the operating band in a nonconservative direction, the alarm system alerts the operator to take corrective action and return the plant to the normal condition. Operation outside the normal range is undesirable because of the reduced margins to safety limits and the possibility of initiating transients from this condition. The technical specifications limit the time during which normal transient adjustments can place the system outside the operating limits. The following paragraphs discuss the normal operating bands for each of the system parameters and the adverse operating limits, including instrument and calibration errors that are used in the safety analyses.

1. Thermal Power Level. The rated power level of the MH-1A is 45 MW thermal. This power level is established by a secondary plant heat balance across the steam generator. The ion chamber current of the power range channels is periodically calibrated to this measured power. Secondary power is obtained from measurement of feedwater flow, feedwater inlet temperature to the steam generator, and steam pressure. Table 2 shows the heat balance

calibration error for nominal full power conditions. These errors are consistent with the specified accuracy of the secondary plant instruments and assume a laboratory-calibrated feedwater flow nozzle. A nominal value of the heat balance calibration error of ±3% is conservatively assumed in the analyses and additional error of ±2% (actual error <1.4%) due to setpoint repeatability is added in determining safety system setpoints. Allowing margin for normal fluctuation in load demand, an alarm placed on power level at 106 percent including allowance for instrument and calibration error, results in an adverse operating power of 111 percent.

2. Primary System Pressure. The nominal primary system pressure at the MH-1A is 1400 psia. The pressure is controlled automatically by three banks of pressurizer heaters and the pressurizer spray valves. During normal operation the first-stage heaters are in continuous operation to offset losses and the second-stage heaters cycle on and off automatically to maintain the pressure between 1385 and 1400 psia. Under transient conditions the third-stage heaters are energized on decreasing pressure at 1355 psia and the pressurizer spray valves are actuated on increasing pressure at 1480 psia. Allowing for transient overshoot and considering that during normal operation the third-stage heaters are not energized, an alarm established on low system pressure at 1340 psia (1325 psig), including allowance for error of ±23 psi, results in an adverse operating pressure of 1317 psia.

3. Reactor Coolant Temperature. The average reactor coolant temperature at rated power is maintained at approximately 490°F during normal full power operation with a corresponding reactor outlet temperature of 506°F. Primary system response to load change during normal operation can result in an increase in coolant temperature at reduced plant load. An operating limit placed on high coolant outlet temperature of 530°F (to provide adequate margin during maximum system load changes) including an allowance of ±4°F for instrument error results in a maximum adverse outlet temperature of 534°F.

4. Primary Coolant Flow. The nominal primary coolant flow at the MH-1A is 10,800 gpm (4.40×10^6 lb/hr at 490°F) based on pump manufacturer test data and plant differential pressure measurements. Uncertainty in the determination of the flow including an allowance for changes in operating characteristics with lifetime results in a minimum normal flow of 10,200 gpm. Small changes in coolant temperature do not affect the volumetric flow significantly.

During normal operation the flow is not controlled by the operator; however, if a reduction or loss of flow were to occur while the reactor is at substantial power, the safety system assures reactor shutdown before DNB limits are reached. The minimum design coolant flow rate assumed in the safety analyses resulting from a reduction in pump output is 8650 gpm. Thus, an adequate margin is provided between the design coolant flow and the minimum normal flow of 10,200 gpm.

TABLE 2

HEAT BALANCE CALIBRATION ERROR IN THE DETERMINATION OF REACTOR THERMAL POWER

Parameter	Secondary Plant Measurement Error	Equivalent Accuracy, % Rated Power
Feedwater temperature	±5.5°F	±0.7%
Feedwater pressure	±16 psia	
Steam pressure (small correction to enthalpy)	±16 psia	
Feedwater flow	±1.25%	±1.25%
	Total error	±1.95%

C. Safety System Setpoints

The reactor safety system automatically trips the reactor to protect the core if measured reactor variables exceed the safety system setpoints. These setpoints are specified so as to assure that none of the core safety limits identified in the thermal hydraulic analysis are violated during either normal plant operations or anticipated transients. Adequate margins are provided between the nominal steady-state operating conditions and the safety system setpoints to prevent spurious scram during normal operation.

Table 3 summarizes the limiting reactor safety system setpoints required by the safety analyses and the effects of instrument and calibration errors on each. The manner in which these setpoints assure protection of the core during steady-state and transient operation and the margins that they provide with respect to the safety limits are discussed in the following paragraphs.

TABLE 3. MH-1A CORE 5 STEADY-STATE SUMMARY

	Power % 45 MW		Flow gpm/psi		High Pressure psia		Low Pressure psia		Outlet Temperature °F	
	w/ error	meas	w/ error	meas	w/ error	meas	w/ error	meas	w/ error	meas
Single Variable Safety Limit	118(1)		7400		1760		1220		546	
Limiting Safety System Setting	115	≤110	8650	≥83%	Safety Valve 1621	≤1600	1267	≥1290	534	≤530
Adverse Limit Operating Band	111	≤106(2)	8650	≥83%	Spray Valve 1500	≤1480	1317	≥1340(2)	534	≤530
Nominal	103	100	10200	100%	1423	1400	1377	1400	510	506

(1) Thermal overpower limit changes with core burnup. Limiting safety system setting is reduced to maintain adequate margin to this limit.

(2) Limiting alarm setpoint specified in technical specification.

1. Steady-State Evaluation. To illustrate the normal margins during steady-state operation or slow transients in which instrument response considerations are not significant, safety limits are determined for single parameters with other variables at their maximum adverse conditions defined above. These represent limits of departure from nucleate boiling (DNB) or void fractions that fall on the more general safety-limits curves. During rapid transients, detailed system response must be evaluated to determine whether an actual safety limit has been exceeded.

a. Reactor Thermal Power. The high reactor power-level trip provides protection against overpower conditions that could result in exceeding limits on fuel temperature or DNB. The effects of fuel densification have been included in the evaluation of these limits. Fuel densification can result in increased local power density and reduced pellet-to-clad thermal conductance, which increases fuel temperature and heat flux during operation. In order to assure that the fuel center temperature does not reach the UO_2 melting temperature, limits have been placed on reactor thermal power level and power-level trip setting as shown in Table 4. The specified safety system setting with allowance for error assures that the safety limits on thermal power level will not be exceeded. These limits consider the variation of fuel temperature and power distribution with burnup. For a given power density, fuel temperature will first increase due to fission gas buildup and then decrease due to irradiation-induced fuel swelling. Therefore, the core power limit and limiting safety-system setting change accordingly.

The changes in the power-level trip setting will be done in a series of discrete steps at intervals determined on review and approval of the plant safety committee following the limits shown in Table 4.

TABLE 4. THERMAL POWER LIMITS VS FUEL BURNUP

Fuel Burnup, Effective Full Power Weeks	Limiting Safety System Setting, % 45 MW_t	Safety Limit, % 45 MW_t
0 to 5	≤ 110	118
5 to 10	105	117
10 to 20	100	110
20 to 30	96	105
30 to 50	94	103
50 to 60	96	105
60 to 70	102	112
> 70	110	118

b. Reactor Coolant Temperature. The high coolant-outlet temperature scram protects the core against DNB or excessive void formation. The analysis shows that the safety limit on coolant temperature during operation within the design limits in 546°F. The reactor scram setpoint of 530°F thus provides a steady-state margin of 16°F before the safety limit is reached; 4°F of this margin accommodates instrument and calibration error.

c. Primary System Pressure. The low-pressure reactor scram protects the core against excessive core void fraction that could result in DNB. The safety limit on system pressure during operation within the design limits is 1220 psia. Thus, the setpoint on primary system low pressure of 1290 psia provides a steady-state margin of 70 psia to the safety limit; 23 psi of this margin accommodates instrument and calibration error.

d. Primary Coolant Flow. This trip protects the core from DNB as a result of decreasing primary coolant flow. The limiting coolant flow rate for steady-state operation is 7400 gpm. The minimum coolant flow assumed in the safety analyses resulting from a reduction of pump output is 8650 gpm. Thus, the steady-state margin between the design flow rate and the safety limit is 1250 gpm.

Low coolant flow in the primary system is sensed by measurement of pump differential pressure and pump power. The low flow trip point is determined assuming a relationship between coolant flow and differential pressure:

$$\frac{dp}{dp_o} = \left(\frac{W}{W_o}\right)^2$$

where dp_o is the reference pressure differential corresponding to the reference flow rate W_o at normal operating conditions. The maximum setpoint error is ± 3.3 psi or 6.2 percent flow including allowances for ship's motion (roll and pitch) and transmitter temperature change. The required setpoint on flow is then (8650/10200) + .062 = 0.91 normal flow or $(.91)^2 100$ = 83 percent normal pressure differential at power (490°F).

Measured pump power under normal operating conditions (490°F) is 189 kw. If one pump becomes inoperable, the maximum power drawn is 113 kw. Thus, a pump power setpoint of 135 kw including effects of instrument error (±4 kw) assures that a reactor scram signal is initiated upon loss of power to one or both primary coolant pumps.

2. Transient Evaluation. A summary of the limiting reactor transients and the protection provided by the safety system is presented in the following paragraphs. The transients are assumed to be initiated from the most adverse initial steady-state conditions so as to minimize the initial margins to DNB. It should be noted that during transient conditions, safety margins are evaluated with respect to safety limits curves. This is the result of the fact that safety limits are related to interdependent variables such as (1) reactor coolant temperature (2) heat flux (thermal power), and (3) reactor coolant pressure. The use of safety-limits curves aids in the determination of whether a particular limit is approached or exceeded.

a. Power Range Rod Withdrawal Transient. The analysis shows that uncontrolled rod withdrawal in the power range for both fast and slow reactivity insertion rates is constrained by a combination of high power and high coolant-outlet temperature scrams. The high power-level scrams provide protection for rapid reactivity insertion rates causing the power level transients too fast for system process variables to respond. The specified setpoints assure that the reactor is scrammed before limits on fuel temperature or DNB are exceeded. The high reactor outlet temperature scram protects the core against uncontrolled slow reactivity insertion or large load mismatch between the reactor and the turbine generator. The analysis shows that the specified setpoint with allowance for instrument response and coolant transport delay (~4 sec) assures that the reactor parameters are always below the core safety limits.

b. Main Steam Line Rupture Transient. The effect of rapid cooldown of the primary system resulting from a main steam line rupture was analyzed for the most severe conditions with respect to reactivity addition and initial steady-state conditions. A minimum pressure corresponding to the low-pressure setpoint plus error was assumed in the analysis because of the rapid decrease system pressure during the transient. The analysis shows that the high-power reactor trip is sufficient to prevent violation of the core safety-limit boundaries.

c. Loss of Coolant Flow. Loss of coolant flow in the reactor loop is sensed by pump differential pressure and pump power. The specified low-flow reactor scram setpoints including error assure protection against DNB in the event of either a decreasing actual measured flow or sudden loss of power to one or both reactor coolant pumps. The analysis shows that the core is protected from loss of flow incident to the specified setpoints and a delay time between pump failure and initial rod insertion of 0.5 seconds. Since any possible increase in measured coolant outlet temperature occurs after the low-flow scram, and since there is no reactor power increase in the transient, the setpoints of these variables are not influenced. While the primary system pressure might increase during the transient, the pressure is conservatively taken at its minimum operating value.

d. Source Range Rod Withdrawal Transient. Protection against rapid approach to criticality caused by continuous control rod withdrawal from a subcritical condition is provided by the high-power reactor trip. Although very conservative assumptions were used, the analysis indicates that the reactor core is fully protected from the source-range rod withdrawal transient. Because of the rapidity of the transient and the long fuel-heat transfer-time constant, fuel temperature is the most limiting safety criterion. There is a large margin to DNB during the transient, since the rod surface heat flux remains low. The maximum fuel temperature during the transient is less than fuel temperatures at rated power. Since the transient is initially terminated by Doppler effect, the fuel temperature is relatively insensitive to reactor power setpoint. The other reactor system setpoints are not influenced by this transient.

III. DESIGN BASES

The thermal design of the MH-1A is based upon protection of the core from any transients or operating conditions that might result in loss of the first line of containment - the fuel-pin cladding. In order to insure that the cladding integrity is not violated, certain design bases are defined. These constitute limits on minimum DNB ratio, maximum fuel-centerline temperature, and flow stability.

A. Departure From Nucleate Boiling Ratio (DNBR).

While the occurrence of DNBR does not necessarily lead to cladding failure, protection against DNB combined with protection against high cladding temperature does insure against cladding failure.

In order to insure that sufficient margin to DNB always exists during steady-state and transient operation, a minimum DNBR of 1.30 was established. DNB ratio is defined as:

$$DNBR = \frac{q''DNB}{q''act}$$

where q"DNB is the heat flux which results in departure from nucleate boiling for given flow rate and core inlet temperature conditions, and where q"act is the actual heat flux for the same flow rate and inlet temperature conditions.

The empirical correlation used to calculate DNB heat flux was Westinghouse W-3 correlation developed by Tong (Reference 3)[1]. The correlation is:

$$q''_{DNB,EU} = [(2.02 - 0.0004302p) + (0.1722 - 0.0000984p) \exp (18.177 - 0.004129p)X] \times [(0.1484 - 1.596X + 0.1729X|X|)G/10^6 + 1.037] \times (1.157 - 0.869X) [0.2664 + 0.8357 \exp (-3.151 D_e)] \times [0.8258 + 0.000794 (H_{sat} - H_{in})].$$

where:

D_e = hydraulic diameter

p = pressure

X = quality

G = mass flow rate

---

[1] L. S. Tong, "Prediction of Departure from Nucleate Boiling for an Axially Non-uniform Heat Flux Distribution, " J. Nuclear Energy, Vol 21, (1967).

H_{sat} = saturation enthalpy

H_{in} = inlet enthalpy

The heat flux is given in Btu/hr-ft^2 and the units and the ranges of parameters of the data used in developing this correlation are:

P = 1000 - 2300 psia

G = .37 x 10^6 - 5.0 x 10^6 lb/hr-ft^2

D_e = 0.2 - 0.7 in.

X_{loc} = 0.15 - +0.15

H_{in} = $\geq$ 400 Btu/lb

channel length = 10 - 144 in.

The correlation is extended to channels with nonuniform axial flux distribution by:

$$q''_{DNB,N} = q''_{DNB,EU}/F,$$

where:

$q''_{DNB,EU}$ = equivalent uniform DNB flux, and

$$F = \frac{C}{q''_{local}[1 - \exp(-C\ell_{CNB,EU})]} \int_0^{\ell_{DNB}} q''(z) \exp[-C(\ell_{DNB} - Z)]dz$$

$$C = \frac{0.15\ (1-X_{DNB})^{4.31}}{(G/10^6)^{0.478}},\ in^{-1}$$

where ℓ_{DNB} = length along channel to the point where DNB occurs.

B. Fuel Temperature.

While it has been proven possible to operate safely with centerline fuel melting (Reference 14)[1], a limit of no centerline fuel melting is placed on the MH-1A to preclude the possibility of cladding damage due to fuel slump. This limit, coupled with the limit on DNBR and the possible range of coolant

1 "High Performance UO_2 Program Molten Fuel Rod Operation to High Burnup," Lyons et al, GEAP-5100-2, November 1966.

temperatures, also precludes the possibility of the cladding temperature's getting high enough to cause either cladding melting or a metal-water reaction. This limit of no centerline fuel melting is expressed as a maximum permissible linear heat rate, which is primarily a function of the thermal conductivity of the fuel.

The UO_2 thermal conductivity is based on the data of Lyons (Ref 4, 5)[1] for 95% theoretical dense fuel:

$$k_{(T)} = \frac{38.2}{129 + T} + 6.126 \times 10^{-13}\ T^3,\ w/cm$$

where $k_{(T)}$ is the fuel conductivity and T is the fuel temperature in °K. The above equation results in an integral $\int k(T)dt$ from 0 to 2800°C of 93 w/cm. The UO_2 melting temperature (Ref 13)[2] is taken as 5080°F unirradiated decreasing by 58° per 10,000 MWD/MTU of fuel burnup.

C. Flow Stability.

Periodic oscillations or instabilities could, if they occurred, lead to coolant conditions that would initiate premature DNB. Instabilities presently postualted depend on the large density changes inherent in a violently boiling environment. During normal operation, the MH-1A does not experience any bulk boiling in the hot channel. During adverse operating conditions the maximum core void fraction is limited to 0.32. This limit is considered conservative in preventing flow instabilities. The computer codes used in the analysis of transients are able to detect and analyze density and friction-factor-driven instabilities. Again, the proper choice of safety system setpoints will preclude any unstable flow oscillations.

---

[1] M. F. Lyons, et al, "UO_2 Pellet Thermal Conductivity from Irradiation with Central Melting", GEAP-4624, 1964.

[2] S. Y. Ogawa, E. A. Lees, and M. F. Lyons, "Power Reactor High Performance UO_2 Program", GEAP-5591, 1968.

[3] J. S. Christensen, J. J. Allio, A. Biancheria, "Melting Point of Irradiated Uranium Dioxide," WCAP-6065, Westinghouse Atomic Power Division, February 1965.

IV. STEADY-STATE ANALYSIS

The purpose of this section is to describe the thermal hydraulic characteristics of the MH-1A core during normal steady-state operation, and to determine the margins between normal operating conditions and those necessary to cause possible fuel-element damage. The steady-state thermal performance of the core is measured with respect to the design criteria discussed in Section III of this report. These criteria constitute limits on minimum departure from nucleate boiling (DNB) ratio, maximum fuel temperature and coolant void fraction. In analyzing the reactor core, the concept of the hot channel is used. This concept assumes that the most adverse fuel-rod properties and channel dimensions occur at the location of the limiting heat flux and coolant flow. This results in one channel in the core being most limiting. The thermal hydraulic performance of the core is measured from the behavior of this hot channel.

A. Operating Parameters.

The total primary coolant flow through the reactor at nominal operating pressure and temperature is 4.40×10^6 lb/hr. A portion of this flow (8.8%) passes through the inner thermal shields and control-rod channels, and is considered coolant leakage flow. The coolant flow area associated with the effective flow is 5.22 ft^2, resulting in an average core-mass velocity at nominal conditions of 0.769×10^6 lb/hr-ft^2. The average core-mass velocity at design conditions is $.604 \times 10^6$ lb/hr-ft^2.

Normal primary system pressure is 1400 psia. Operating band and instrument error associated with pressure result in range in actual pressure between 1317 psia and 1500 psia. The nominal full-power core inlet temperature is 476°F. Maximum coolant inlet temperature is 492°F corresponding to an outlet temperature of 534°F. Table 5 shows the operating parameters for the nominal and design conditions used for the steady-state analysis of Core 5.

TABLE 5

MH-1A CORE 5 THERMAL HYDRAULIC OPERATING PARAMETERS

	Nominal	Design
Reactor power, % 45 MW_t	100	111
Primary system flow rate, lb/hr	4.40×10^6	3.46×10^6
System pressure, psia	1400	1317
Coolant inlet temperature, °F	476	492

B. Hot-Channel Factors.

In evaluating the thermal-hydraulic performance of the core, the local increase of heat generation and enthalpy rise with respect to the core average value is accounted for by the use of hot-channel factors. Two types of hot-channel factors are considered: Nuclear hot-channel factors, which describe the neutron flux distribution in the core, and engineering hot-channel factors, which account for local variations in fuel-rod properties due to fabrication tolerances. Sources of engineering hot-channel factors are tolerances on fuel-pellet diameter, enrichment, and density and fuel-rod loading. The influence of variations in rod diameter, pitch, channel area, and rod bowing are accounted for by direct use of adverse dimensions in the analysis. Hot-channel factors for heat flux or linear power depend on local properties (hot spot), and factors for enthalpy rise consider the integrated effect along the length of the channel (hot channel). The overall hot-channel factors on heat flux or enthalpy rise are the product of the appropriate individual subfactors.

1. Engineering Hot-Channel Factors and Dimensional Considerations. Hot-channel engineering factors used in the analysis of Core 5 are derived from the appropriate tolerances in the fuel-rod specifications (Reference 7)[1]. The engineering factor on enthalpy rise is taken as the ratio of the maximum U-235 loading to the nominal for a fuel rod (1.02). Engineering factors for local power or heat flux are determined from the tolerances on the UO_2 fuel enrichment, density, and fuel diameter, and the combined total factor is 1.03.

The effect of variations in channel dimensions on enthalpy rise and local DNB heat flux are incorporated directly into the analysis. Channel-flow area and hydraulic diameter are determined from the fuel-rod pitch. The effective minimum fuel-rod pitch depends on several factors, which include the tolerances on the base-plate holes and end caps, assembled fuel-rod bowing tolerance, and possible thermal bowing due to a temperature gradient across the fuel rod. The minimum fuel-rod pitch resulting from these sources was found to be 0.615 inches with a corresponding reduction in flow area from .226 to 0.176 in^2.

The inlet flow distribution in the region of the hot channel has maximum effect on channel-enthalpy rise of 1.02. Flow redistribution resulting from increased resistance due to local boiling reduces the flow in the hot channel. A nominal value for this subfactor is 1.06, although in the analysis each case is calculated individually. The analysis also considers thermal mixing between adjacent flow channels. Mixing tends to decrease the hot-channel enthalpy rise by redistributing flow to the cooler adjacent channels. The mixing effect increases with increasing distance above the core inlet. A nominal mixing factor to the elevation of minimum DNB ratio is 0.91, although each case is computed individually in the analysis.

2. Nuclear Power Distribution. The core distribution is primarily determined at the beginning of core life by such parameters as fuel enrichment,

[1] "Specification for Fuel Element Assemblies of the MH-1A Type II Core", NYO 10748, New York Operations Office, June 1970.

burnable-poison placement and control-rod worth but also changes during operation due to Xenon buildup and depletion effects. Two types of power peaking are of interest to the thermal analysis: 1) core radial enthalpy-rise distribution and 2) the maximum core heat flux. The enthalpy-rise factor is defined as the ratio of maximum integral power of fuel rods surrounding the hot channel to core average integral rod power. The design enthalpy-rise factor is 1.67 based on an effective integrated power established from radial power distribution in the rodded and unrodded region of the core at the beginning of core life. These do not change appreciably with core burnup.

The heat-flux factor is defined as the ration of maximum heat flux in the core to the average value. This peaking factor is a combination of axial and radial power distributions in the core and is sensitive to the control rod bank position and Xenon distribution. The maximum value of the radial and axial peaking combined as determined in the nuclear analysis (Reference 11)[1] is 1.84 x 1.76 = 3.24 at the beginning of core life. This value is conservatively used in the evaluation of DNB although it significantly decreases with Xenon buildup and burnup. In evaluating fuel temperatures, the effects of fuel depletion and Xenon distribution are considered in the analysis. The hot-channel factors for heat flux and enthalpy rise are summarized in Table 6.

---

[1] Hollis, H. D., et al., "The Theoretical Nuclear Analysis of the MH-1A Core 5", ED-7211, USAENPG, 10 July 1972.

TABLE 6

HOT-CHANNEL FACTORS FOR DEPARTURE FROM NUCLEATE BOILING (DNB) AND ENTHALPY-RISE CALCULATIONS

F_Q^N	Nuclear heat-flux factor	3.24
	Uncertainty	1.10
F_Q^E	Pellet diameter, enrichment, density	1.03
	Rod Diameter	
	Total	3.67
$F^N_{\Delta H}$	Nuclear enthalpy-rise factor	1.67
	Uncertainty	1.05
$F^E_{\Delta H}$	U^{235} loading	1.02
	Rod diameter, pitch, thermal bowing	1.28
	Inlet flow maldistribution	1.02
	Flow redistribution	1.06
	Flow mixing	0.91(1)
	Total	2.25

(1) To point of minimum DNB ratio.

C. Method of Analysis.

1. Fuel Temperature. The steady-state fuel temperature distribution and pellet-to-cladding thermal conductance are calculated using the methods and assumptions outlined in the addendum to this report.

Heat conduction through the clad and gap is calculated to give the fuel surface temperature as a function of power level. The fuel centerline temperature is then determined based on the local heat generation in the fuel and the temperature dependent UO_2 thermal conductivity. The upper limit on the coolant temperature is taken as the saturation temperature at given system pressure. The temperature increment between the bulk coolant and cladding wall is given by the conservative Thom nucleate boiling correlation (Reference 12)[1]:

$$T_w = T_{sat} + .072\ (q'')\ 0.50\ (e^{-P/1260}) \qquad (1)$$

T_w = cladding surface temperature, °F

T_{sat} = saturation temperature for system pressure, °F

q'' = local surface heat flux, Btu/hr-ft

P = system pressure, psia

The heat generation shape in the fuel is represented by a modified zero order Bessel function. The temperature distribution in the fuel is determined from the solution to the heat conduction equation expressed in terms of local heat generation or power density.

$$4\pi \int_{T_s}^{T_c} k(t)dT = q'f \qquad (2)$$

where: q' = peak local heat generation rate

$k(T)$ = thermal conductivity of UO_2

T_s = fuel surface temperature

T_c = fuel center temperature

f = flux depression factor

The flux depression factor (f) accounts for radial distribution of heat generation across the fuel pin, which is based on the U-235 enrichment

---

[1] Thom, J. R. S., W. N. Walker, T. A. Fallon, and G. F. S. Reising, "Boiling in Subcooled Water During Flow Up Heated Tubes or Annuli," Proc. Instn. Mech. Engs. 1965-66, Vol. 180, Part 3C, (1966).

and rod diameter as given in Reference 10[1]. The fuel temperature is computed as a function of linear rod power considering the effects of fuel densification and burnup as discussed in the addendum.

2. Calculation of Enthalpy Rise and DNBR. The basic method used in the analysis of the MH-1A hot-channel enthalpy rise and DNB ratio conditions is the COBRA digital computer program (References 6 & 9)[2]. The COBRA program calculates coolant flow and enthalpy in the subchannels of a multirod bundle. The program has the ability to consider both single- and two-phase flow, and accounts for the flow redistribution and thermal mixing between adjacent flow channels resulting from turbulent cross flow and diversion cross flow. An arbitrary heat-flux distribution can be input by specifying the axial-flux distribution, relative rod power, and the fraction of rod power to the adjacent subchannels.

Differences in hydraulic resistance due to local boiling cause flow redistribution which may increase the hot channel enthalpy rise. COBRA calculates the flow distribution in the subchannels by forcing the pressure drop in each channel to be identical. Turbulent mixing tends to reduce the hot-channel enthalpy rise caused by local power peaking and adverse mechanical dimensions. The effect of turbulent mixing has been previously considered for the MH-1A in Reference 8[3]. A value for the turbulent mixing parameter of 0.0075 was determined to best represent MH-1A subchannel conditions where the correlation for β is written:

$$\beta = 0.0062 \frac{D}{S} (R_e)^{-0.1} \qquad (3)$$

where: D = the hydraulic diameter (inches)

S = the rod spacing (inches) and

R_e = the Reynolds number

COBRA is modified to calculate DNB ratios utilizing the W-3 DNB correlation and calculated channel conditions. The W-3 correlation includes the effect of a nonuniform heat-flux distribution, and takes into account both local and upstream channel properties in determining the local DNB heat flux. The subchannel configuration used in the DNB evaluation is shown in Figure 2. This corresponds to a region at the center of the core near the source-rod position.

---

[1]J. A. L. Robertson, "$\int$kdt in Fuel Irradiations" CRFD-835, Atomic Energy of Canada Ltd., 1959.

[2]D. S. Rowe, "Cross Flow Mixing Between Flow Channels During Boiling, Part 1, COBRA - Computer Program for Coolant Boiling in Rod Arrays", BNWL-371 Pt 1, Battelle Northwest, March 1967.

[2]D. S. Rowe and E. W. Angle, "Crossflow Mixing Between Parallel Flow Channels During Boiling," Pt II Measurement of Flow and Enthalpy in Two Parallel Channels," BNWL-371 Pt 2, Pacific Northwest Laboratory, December 1967.

[3]Meyers, C. A., et al., "MH-1A Steady-State and Transient Thermal-Hydralic Design Analysis," ED-6916, USAERG, 25 July 1969.

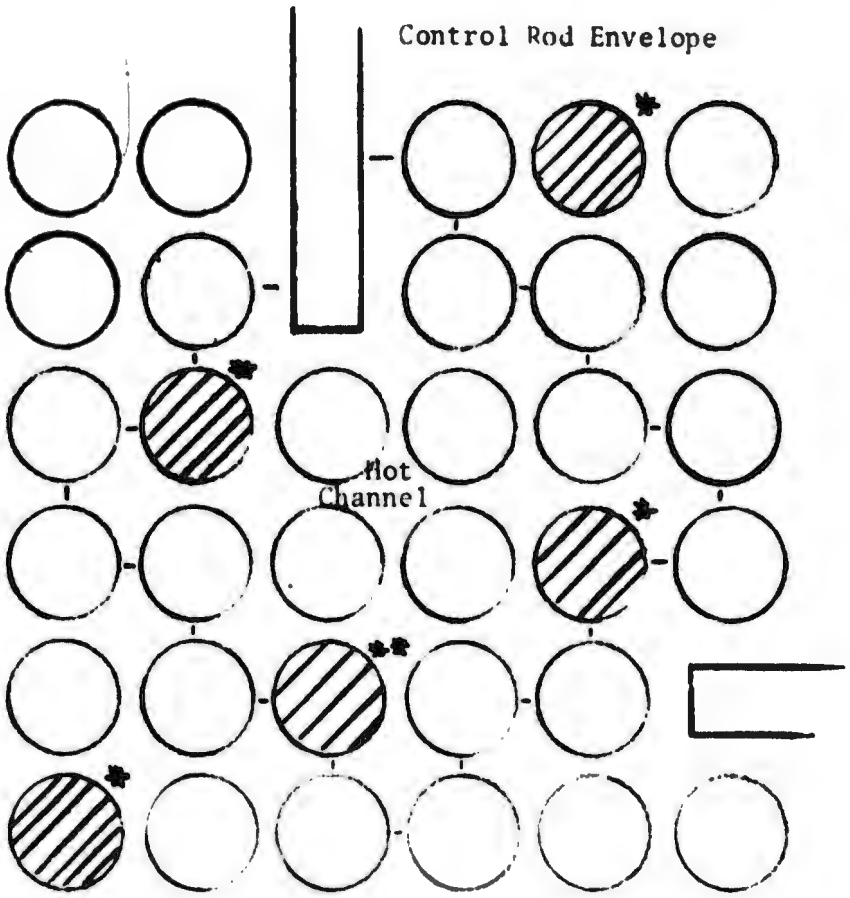

* poison rod

** source rod (core ℄)

FIGURE 2. SUBCHANNEL CONFIGURATION FOR CORE 5 DNB AND ENTHALPY RISE CALCULATION

D. Results.

1. Fuel Temperature Distribution. The temperature distribution from the surface of the fuel to the centerline is primarily a function of UO_2 thermal conductivity and the local power density. The fuel surface temperature is affected by the cladding temperature and thermal conductance across the gap. The occurrence of nucleate boiling results in a cladding surface temperature of less than 612°F for a maximum system pressure of 1500 psia.

Thermal conductivity of the UO_2 was evaluated from the design equation for thermal conductivity presented in Section III of this report. Figure 3 shows the pellet temperature distribution at the beginning of core life for densified fuel. The maximum UO_2 temperature for normal operation at rated power is 4100°F and at the maximum power level trip condition (115% power) is 4400°F. This is well below the UO_2 melting temperature at BOL (5080°F). Changes in fuel temperature and power distribution with core burnup are discussed in the addendum to the report.

2. Enthalpy Rise and DNB. Results of the hot-channel analysis for DNB and coolant void fraction are given in Table 7 for various operating conditions. As can be seen adequate margin is maintained during normal and adverse operating conditions. Further evaluation of safety margins and discussions of safety limits are given in Section II.

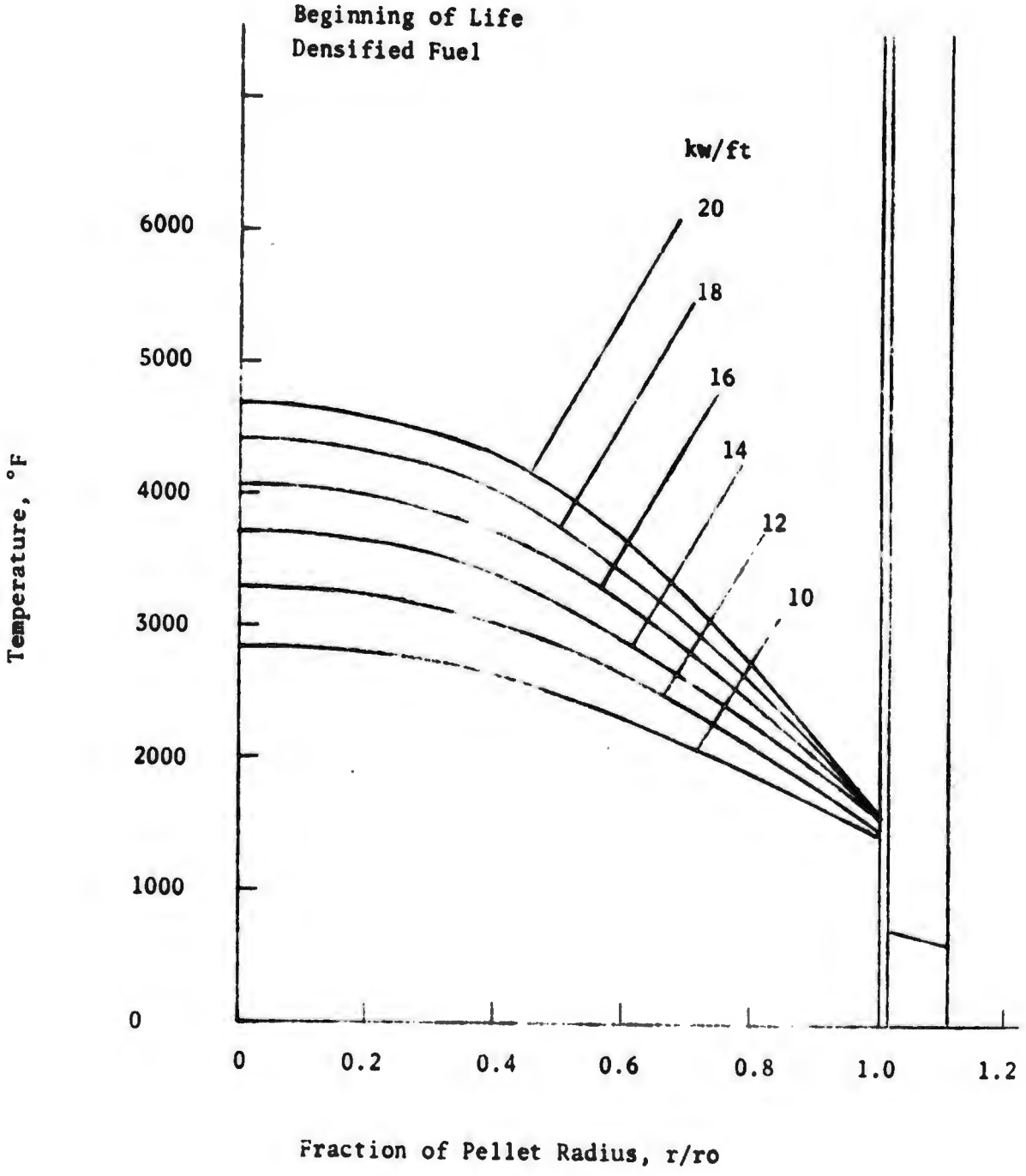

FIGURE 3. FUEL TEMPERATURE DISTRIBUTION

TABLE 7

HOT-CHANNEL CHARACTERISTICS FOR NOMINAL, DESIGN, AND REACTOR TRIP CONDITION

Operating Condition	Power Level % rated	System Pressure psia	Outlet Temp °F	Min DNBR	Max Void Fraction
Nominal	103	1377	510	2.00	0
Design	111	1317	534	1.67	0.13
Trip	115	1267	534	1.59	0.25

V. TRANSIENT ANALYSIS

This section gives a description of the analysis of transients resulting from continous withdrawal of one or more control rods when the reactor is in the power range; double-ended rupture of the secondary system steam line; uncontrolled rod withdrawal during source-level startup; and loss of reactor coolant flow due to loss of power to both pumps. These represent the limiting reactor transients for the evaluation of the reactor protection system and setpoints.

A. Power-Range Rod-Withdrawal Transient.

1. General. It is possible during operation in the power range for the control rods to be withdrawn from the core without an increase in load in the turbine cycle. This causes an initial increase in power, which is slowed down by both the negative temperature coefficient of the coolant and the Doppler coefficient of the fuel. The response of the core is an increase in heat flux. Since there is no corresponding increase in heat extraction from the steam generator, there is a net increase in primary-coolant temperature. Unless terminated by manual or automatic action, this power mismatch and resultant coolant-temperature rise eventually result in violation of the core safety limits. To prevent the possibility of violation of any of the core safety limits, the reactor protection system and trip setpoints are designed to terminate any such transient with an adequate margin of safety.

Since the MH-1A reactor has twelve control rods and since it may be postulated that one or more of these control rods may be withdrawn from the core, there is a spectrum of reactivity insertion rates that are possible during power-range rod withdrawal transient. Thus, both fast and slow reactivity insertion rates are considered to assure that the reactor safety limits are not exceeded.

2. Analythical Methods. The calculation of the power-range rod withdrawal transient was performed in two stages consisting of an average core calculation and then a determination of hot-channel conditions. The method of analysis consisted of the use of the following digital computer codes: DRAKE, CHIC-KIN, and COBRA.

The average core response to the transient was determined using the DRAKE digital computer program, which simulates the overall plant dynamics. The code solves the reactor kinetics equations with six delayed neutron groups. Reactivity introduced by control rod motion can be represented, and feedback reactivity due to moderator temperature and Doppler effect is accounted for. The core is represented by a single nominal channel with four axial zones. Temperatures in the fuel and cladding are calculated assuming a constant volumetric heat source in the fuel region and no axial heat conduction. The model includes a representation of the external primary system, including the steam generator. The hot and cold primary-coolant legs are represented by pure transport delays, and the reactor

vessel and the steam generator plenums are represented by first-order mixing delays. Modeling of the secondary side of the steam generator includes the steam throttle valve, but does not include effects due to the turbine or condenser. Allowable forcing functions for the DRAKE program are steam generator secondary temperature, turbine throttle position, and reactivity insertion. A more detailed description of this program is presented in Reference 8[1].

To determine the conditions in the hot channel, the power trace from the DRAKE program is used as a forcing function in the CHIC-KIN digital computer program (Reference 17)[2]. This program is used for intermediate and fast transients and is especially useful when a detailed analysis of the core thermal response is required. The program solves the basic momentum, continuity, and energy equations. The core model considered by the CHIC-KIN program is represented by a single fuel-element coolant passage where the coolant channel is closed. A detailed spatial representation of the fuel element by axial and radial sections is possible. Representation of the fluid dynamics by a momentum integral model that allows flow reversal and spatially distributed pressure drops is also included in the core model. The heat release from the fuel element is described by one dimensional heat conduction to the cladding water interface where the effect of the fuel rod time delay is included in the energy balance.

The COBRA computer program was used to obtain the initial coolant enthalpy and heat flux conditions in the hot channel.

The following assumptions and input parameters were used in the analysis:

(1) The forcing function for the rod withdrawal transient is the reactivity insertion rate. The maximum rate possible is determined from the 12-rod bank integral-worth curve by combining the maximum differential worth with the rod speed of 2 inches per minute. This results in a conservative maximum reactivity insertion rate of 5.5×10^{-4} dk/sec.

(2) The nuclear constants used in the reactor kinetics equations are given in Reference 11[3]. The prompt neutron lifetime was taken as 1.2×10^{-5} sec in the analysis, and the effective delayed neutron fraction was $\beta_{eff} = .0074$. These values were also used in the analysis of other transients in this report.

---

[1] Meyers, C. A., et al., "MH-1A Steady-State and Transient Thermal-Hydraulic Design Analysis," ED-6916, USAERG, 25 July 1969.

[2] Redfield, J. A., "CHIC-KIN - A Fortran Program for Intermediate and Fast Transients in a Water Moderated Reactor WAPD-TM-479," January 1965.

[3] Hollis, H. D., et al., "The Theoretical Nuclear Analysis of the MH-1A Core 5" ED-7211, USAENPG, 10 July 1972.

(3) The moderator reactivity coefficient varies with average coolant temperature. A conservative minimum value at 490°F of -2.2×10^{-4} dk/°F was assumed. Use of a constant value in the analysis is justified because the coolant undergoes only a small change in temperature during the transient. The Doppler reactivity feedback is a nonlinear function of fuel temperature. The effective initial value at full power used in the analysis was -1.5×10^{-5} dk/°F based on the assumed Doppler coefficient. The assumed reactivity coefficients result in a minimum negative reactivity feedback and therefore, higher peak powers and fuel temperatures.

(4) Negative reactivity insertion corresponding to reactor trip is based on the control rod acceleration and rod bank differential worth. The first 8 inches of rod motion is conservatively assumed to occur within 0.5 seconds. The high-power reactor scram was assumed to occur at 115 percent of nominal full power with a delay of 0.5 seconds.

(5) In order to minimize initial margins to Departure from Nucleate Boiling (DNB) the transients were assumed to be initiated from their adverse operating limits including error.

3. Results.

a. Rapid Reactivity Insertion. Figure 4 shows the response of the nuclear power and core heat flux as a function of time for rapid control rod withdrawal initiated from 103 percent of full power. The reactivity insertion rate assumed (5.5×10^{-5} dk/sec) is greater than the withdrawal of all control rods from their region of maximum worth. It can be seen that a small amount of power overshoot occurs and that the rise in core thermal flux is not appreciable. The termination of the transient was by power level trip. Since the transient is rapid with respect to thermal time constants of the plant, changes in coolant and fuel temperatures are small. The mimimum DNB ratio is 1.73. Increasing the power to 111% results in a mimimum DNBR of 1.66.

b. Slow Reactivity Insertion. For uncontrolled slow reactivity insertion rates, reactor coolant temperature and pressure could increase significantly without causing a scram on high power. During the limiting transient of this nature, is is assumed that the negative moderator temperature feedback just compensates for the reactivity added by rod withdrawal and that the core power increases to just below the trip point (115 percent power). The maximum mismatch between the turbine generator and reactor core is assumed, resulting in a coolant heat-up rate of 1.9°F/sec. The manner in which the high-temperature trip provides protection for the limiting transients is evaluated by considering the maximum temperature overshoot and corresponding pressure increase caused by primary expansion.

FIGURE 4. POWER RANGE ROD WITHDRAWAL TRANSIENT FROM FULL POWER

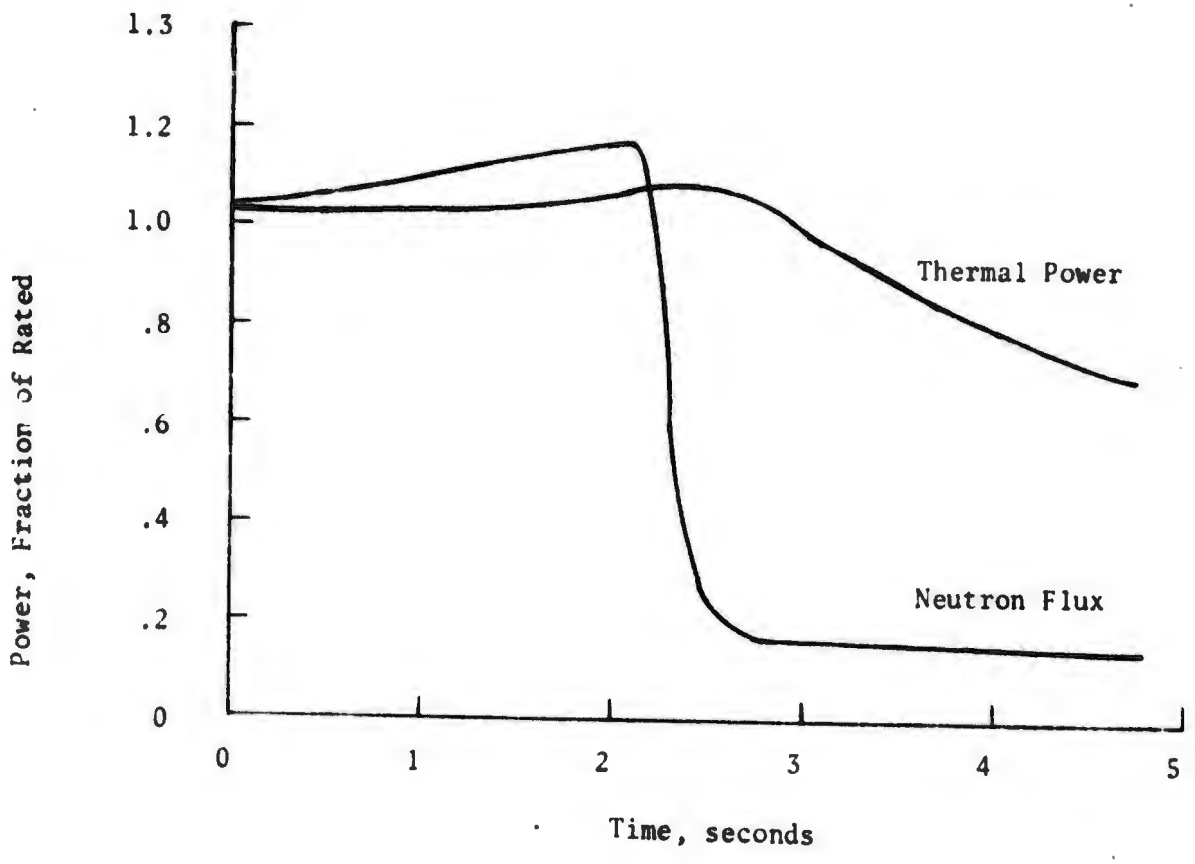

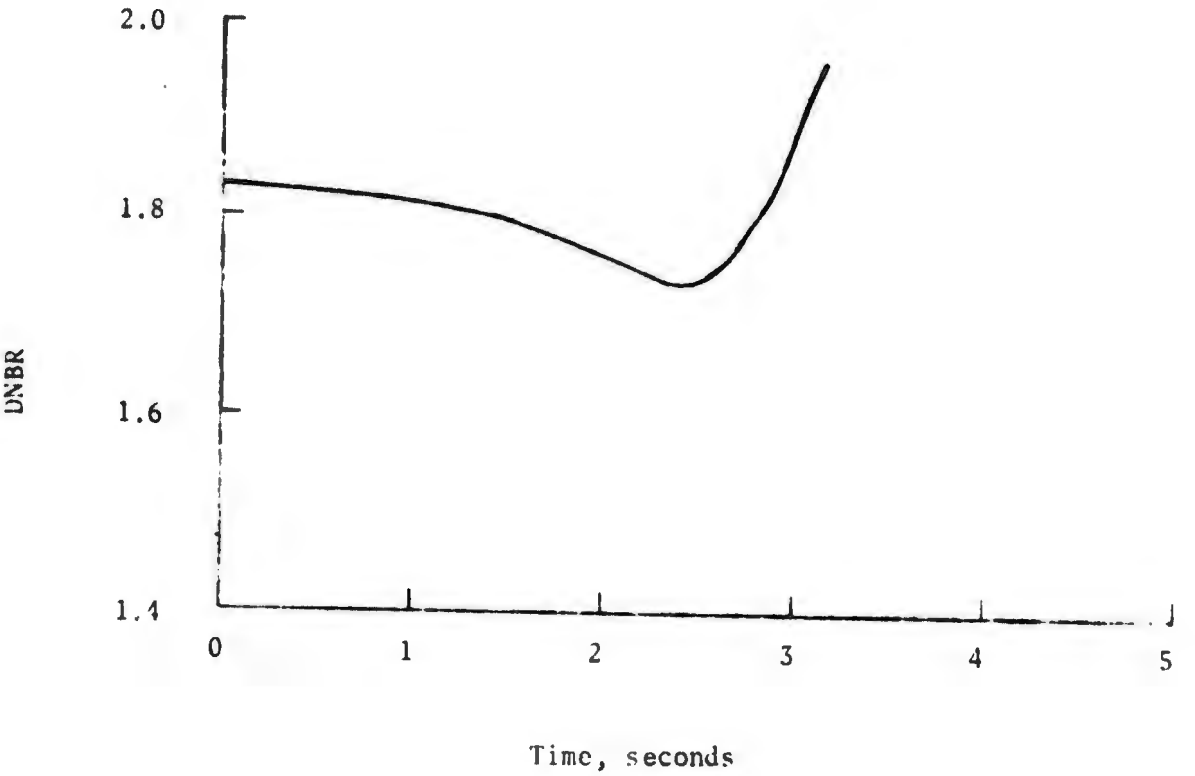

The transient pressure response is calculated using the computer code TOPS (Reference 15)[1]. This code models the pressurizer dynamics based on the primary system surge rate and associated thermodynamic processes in the pressurizer. The effects of pressurizer heaters, cooldown spray, and pressure relief valves as well as heat transfer to the pressurizer walls can be represented in the code. Physical dimensions, heater ratings, spray rates, setpoints and initial conditions are input.

The response of the temperature detector and thermal well is represented by a first-order delay. The lag of the measured temperature with respect to the actual temperature was determined for a constant increase in coolant temperature as:

$$\Delta T_m = -\frac{1}{a}\frac{dT}{dt}(1 - e^{-at}) \qquad (4)$$

where: ΔT_m = difference between measured and actual temperature, °F

$\frac{dT}{dt}$ = ramp change in coolant temperature, °F/sec

a = instrument time constant, sec^{-1}

t = time, sec

The instrument time constant is 0.1 sec^{-1} based on 23 seconds to reach 90 percent step input signal. An additional time lag of 0.5 seconds was assumed for safety system response and clutch decay. The coolant transport delay from the core outlet to the temperature detectors in the hot leg was conservatively taken as 4 seconds.

Figure 5 shows the locus of trip conditions for coolant heat-up transients initiated over a range of initial temperatures up to the maximum (534°F) and from a minimum initial system pressures to 1267 psia. The solid line represents the safety limits on coolant temperature and pressure at a reactor power of 115 percent. The core limits are exceeded if the maximum trip conditions pass above the safety limit line. As can be seen the high temperature trip, including allowance for instrument response and coclant transport delay assures that the core safety limits are not exceeded.

4. Conclusions. The analysis shows that the reactor is protected from the most limiting rod-withdrawal transients resulting from both rapid and slow reactivity insertion rates by a combination of high power and high reactor-coolant outlet-temperature trip. Thus, it is concluded that the reactor can undergo uncontrolled rod withdrawal in power range without violating any core safety limits.

---

[1]Redfield, J. A. and S. C. Margolis, "TOPS - Fortran Program for the Transient Thermodynamics of Pressurizers", WAPD-TM-515, December 1965.

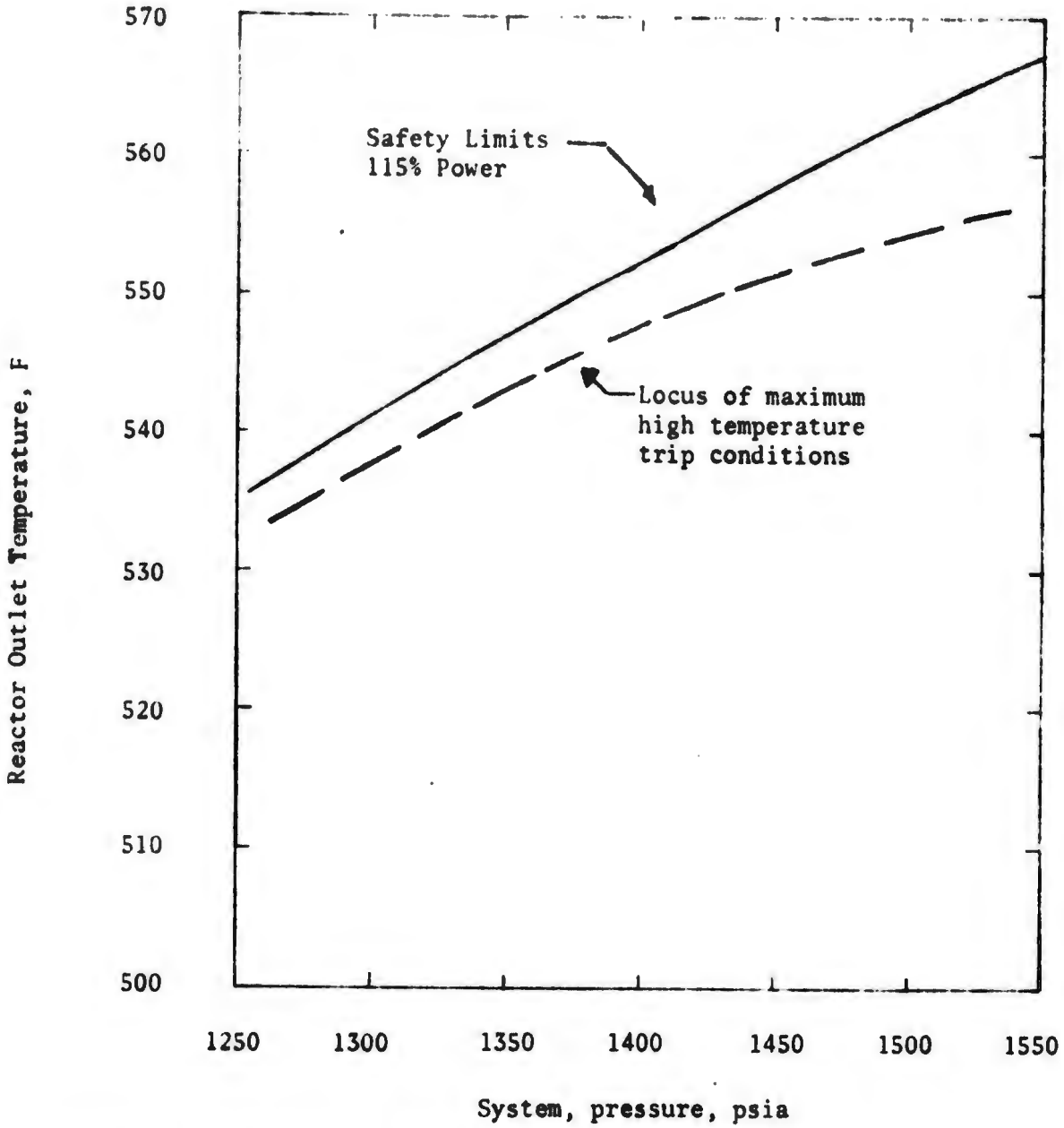

FIGURE 5. HIGH COOLANT TEMPERATURE PROTECTION LIMITS

B. Main Steam Line Rupture Transient (MSLRT).

1. General. The integrity of the turbine-cycle steam system affects the safety of the reactor plant in that a rupture in this system can lead to an increase in the rate of heat transfer of the primary to the secondary system. A steam-line rupture results in a sudden decrease in the secondary-system temperature and pressure due to loss of water and steam through the break, with a resulting loss of energy from the secondary system. This transient is reflected in the primary system as a sudden apparent increase in turbine load, causing a reduction in primary-coolant temperature. The combination of the negative moderator temperature coefficient and the decrease in reactor inlet temperature results in a positive reactivity insertion rate, i.e., in a cold-water transient. This transient results simultaneously in an increase in reactor power due to the reactivity insertion, and a decrease in primary-system pressure due to the reduction in primary-coolant temperature. The increase in reactor power results in an increase in fuel temperature, which via the negative fuel temperature coefficient (Doppler) causes a slowing down, and in some cases, a turn-around and decrease of reactor power. Unless terminated by a manual or automatic action, the increase in power level could result in the violation of one or more of the core safety limits. To prevent this possibility the reactor safety system, along with the trip setpoints, is designed to assure protection of the core with an adequate margin of safety.

2. Analytical Methods. The methods used to analyze the main steam line rupture transient consisted of using a time-dependent decrease of the steam generator secondary temperature as a forcing function in the reactor plant transient code DRAKE, to obtain the reactor power as a function of time. This power profile, in turn, was used in the CHIC-KIN program to determine the hot-channel conditions of minimum DNBR and maximum fuel temperature.

The main steam line rupture is simulated by an exponential decrease of the secondary temperature using a decay constant of 3.0 seconds. Previous calculations of the MH-1A steam line rupture blowdown transient (Reference 8)[1] demonstrated that this representation of the secondary temperature is conservative. These calculations were performed with a digital computer program, which describes the time-dependent secondary system temperature and pressure by calculating mass and energy balances during the blowdown of the secondary-side contents following the rupture of the main steam line.

The version of the DRAKE program employed in the analysis includes a simulation of the external primary loop, including the steam generator. The hot and cold primary coolant legs are represented by pure transport delays, and the reactor vessel and steam generator plenums are represented by first-order mixing delays. The steam generator is treated as a lumped parameter system, and the steam generator heat transfer coefficient is assumed to be a function of the heat flux. A more detailed description of this program is reported in Reference 8.

---

1 Meyers, C. A., et al., "MH-1A Steady-State and Transient Thermal-Hydraulic Design Analysis," ED-6916 USAERG, 25 July 1969.

The principal assumptions and input parameters used in the analysis of the main steam line rupture transient were:

(1) The moderator temperature coefficient was taken as a conservatively large negative value (-3.3×10^{-4} dk/°F), resulting in the maximum reactivity insertion due to the decreasing coolant temperature. A constant coefficient was used throughout the transient although the actual coefficient would decrease as a function of temperature. A small negative Doppler coefficient was used in the analysis (-1.5×10^{-5} dk/°F at full power). These assumptions are conservative because they result in a higher net reactivity insertion rate and thus a more severe power excursion.

(2) The nuclear parameters described in Section V-A were assumed for the reactor kinetics equations. A high power level trip including error of 115 percent was used along with a conservative delay of 0.50 seconds.

(3) The most adverse steady-state conditions were assumed to exist just prior to the transient in order to minimize initial safety margins. Full-load (103 percent power) and no-load (0.1 percent power) conditions were analyzed. Since the primary coolant temperature and hence system pressure decreases very rapidly during the transient, a system pressure of 1267 psia (trip setpoint plus error) was conservatively assumed.

3. Results. The main steam line rupture transient was initiated from power levels of 0.1 and 103 percent. The response of the reactor system to the transient initiated from 0.1 percent power is shown in Figures 6 and 7. Figure 6 shows both the exponential decrease of the secondary temperature used as a forcing function for the transient, and the corresponding changes in the steam-generator primary-coolant temperature and reactor inlet temperature obtained from the DRAKE program as a function of time after the initiation of the transient. Note that the response of the reactor inlet temperature lags that of the steam generator outlet temperature due to the mixing and pure transport delays in the primary system piping.

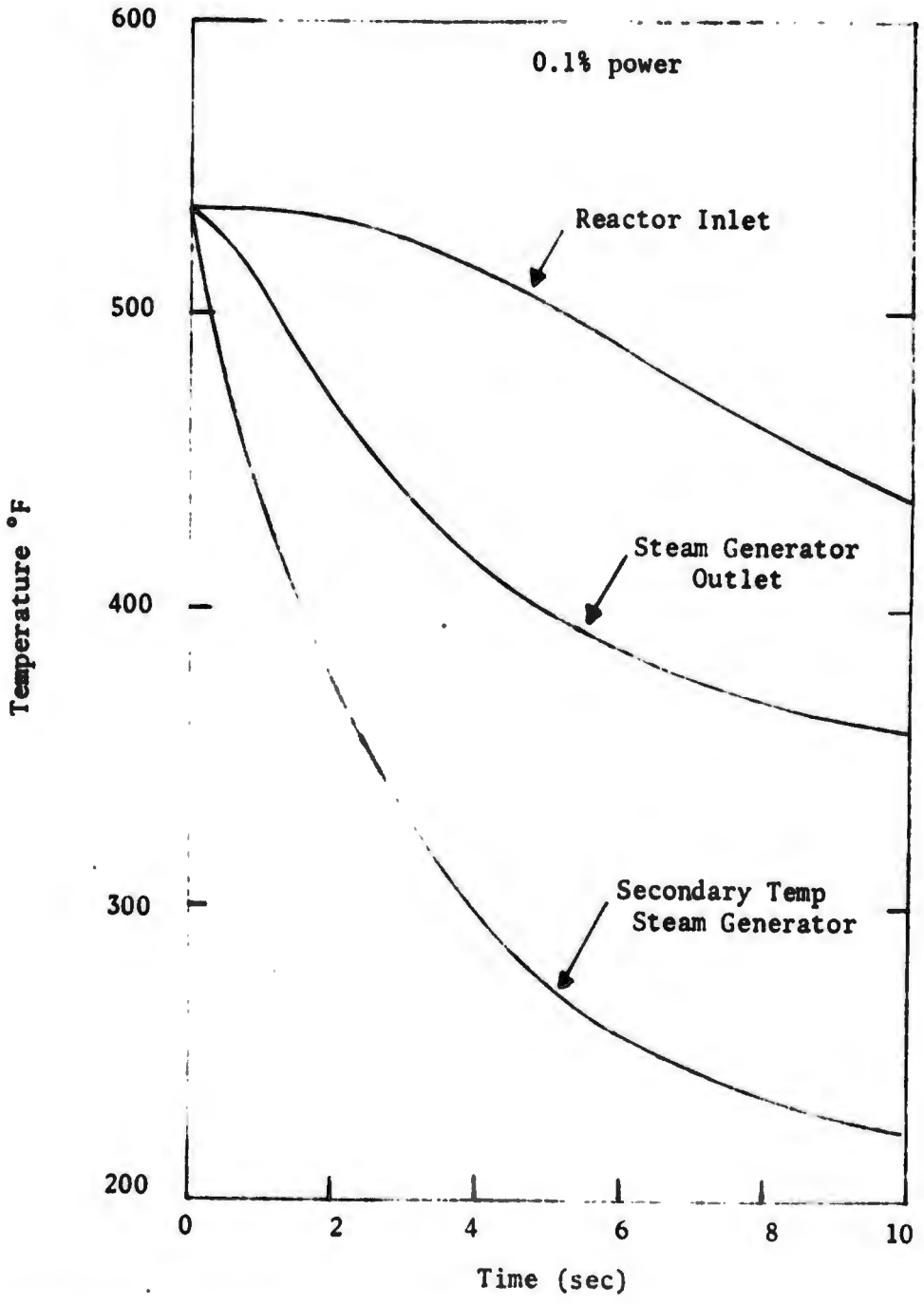

FIGURE 6. MAIN STEAM LINE RUPTURE COOLANT TEMPERATURE RESPONSE

Figure 7 shows the variation of neutron power and heat flux during the transient initiated from zero-load condition. The positive reactivity inserted by decreasing reactor inlet temperature caused the reactor neutron flux to increase rapidly since there is no significant fuel-temperature (Doppler) reactivity feedback. After the power level has risen above approximately 10 percent, the sudden increase in fuel temperature partially compensates for the reactivity added by the decreasing inlet temperature. The power excursion is turned around by the negative Doppler feedback. The core heat flux lags the neutron power level because of the relatively long fuel time constant associated with the oxide fuel. The maximum core heat flux reached prior to trip is less than the full-power flux.

The response of the reactor to the transient initiated from 103 percent power level is shown in Figure 8. For this transient the reactor power increases slightly until the plant is scrammed on high neutron flux. The heat flux again lags the power level, and the increase in fuel temperature and power level are relatively small. The minimum Departure from Nucleate Boiling Ratio (DNBR) was 1.72. Increasing the initial power to 111% results in a minimum DNBR of 1.65.

4. Conclusions. Since the analysis demonstrates that no core safety limits are violated during these transients, it is concluded that the reactor can undergo the most limiting steam-line rupture transients without damage to the core.

C. Source-Range Rod Withdrawal Transient.

1. General. In the unlikely event of an uncontrolled rod withdrawal while the reactor is in a subcritical condition, a continuous reactivity insertion and increase in multiplication would occur. The reactor response to this reactivity insertion is characterized by rapid increase in neutron flux terminated by Doppler fuel temperature feedback. Although initial turnaround of the power excursion occurs as a result of negative Doppler reactivity feedback, reactor protective action by high power trip is required to assure that a subsequent slower increase in power will not cause violation of core safety limits.

2. Method of Analysis. An extensive analysis of the source-range rod withdrawal incident was performed for Type I fuel and reported in Reference 18[1]. In these studies the initial flux level was approximately nine decades below full power. The study included investigation of the effects of hot and cold initial core conditions, initial subcriticality, reactivity insertion rate, and Doppler reactivity feedback. Additional analyses of the transient were performed for the Type II fuel using the CHICK-KIN computer program. In these analyses the reactor was assumed to be critical at 13 decades below full power at 490°F. The reactivity insertion corresponding to withdrawal of all rods (5.5×10^{-4} dk/sec) was assumed with a temperature dependent Doppler coefficient as described previously. These assumptions resulted in the most severe power excursion for the Type II fuel.

---

[1] R. D. Caw, et al, "MH-1A Analog and Controls Analysis" Martin Company, Nuclear Division, 19 Feb 1965.

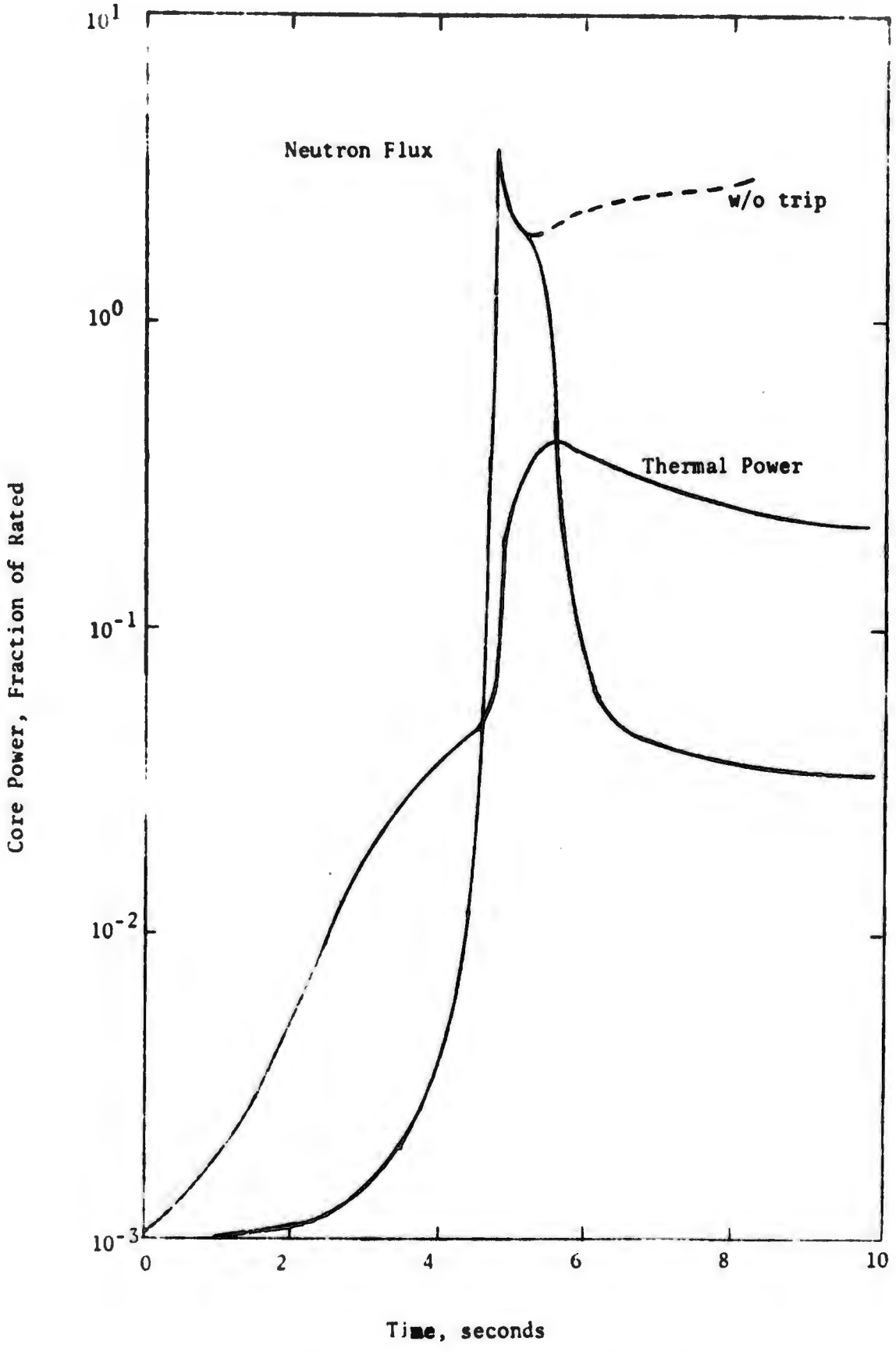

FIGURE 7. MAIN STEAM LINE RUPTURE FROM 0.1% POWER

FIGURE 8. MAIN STEAM LINE RUPTURE TRANSIENT FROM FULL POWER

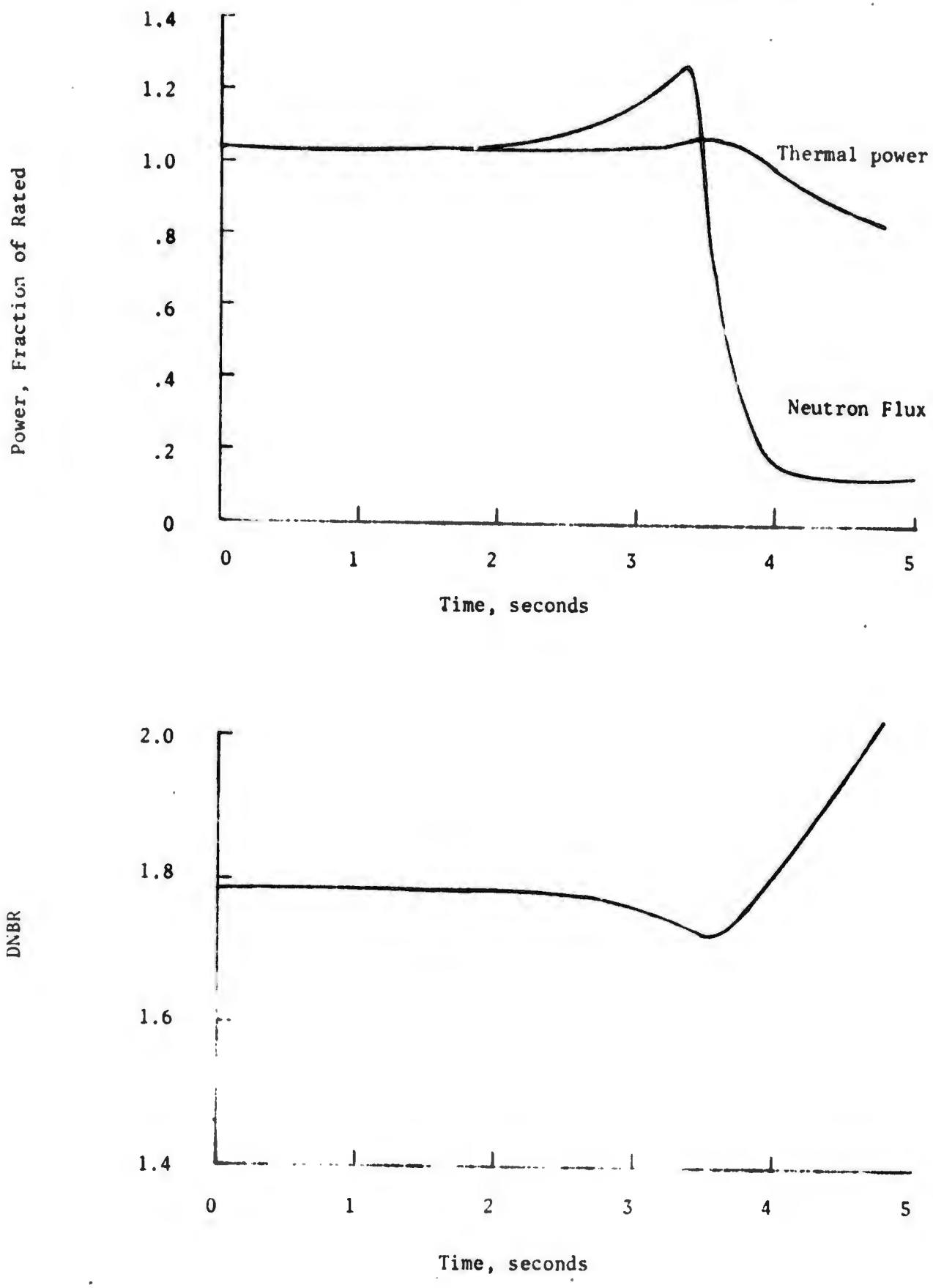

3. Results. Figure 9 shows the results of the source-range rod withdrawal transient for the maximum reactivity insertion rate of Core 5. The peak neutron flux is less than 300 percent. Due to the large time constant of the fuel rod and the short duration of the peak, no significant amount of heat is transferred to the coolant. Thus, DNB conditions are not approached because the rod surface heat flux remains low. Due to the short duration of the power peak, the integrated heat input to the fuel elements is small. The average fuel temperature for Core 5 was found to be less than 800°F.

Figures 10 and 11 show results of the parametric studies performed for Type I fuel considering the effects of subcriticality and Doppler coefficient. Since the Doppler coefficient for Core 5 falls between the mimimum and expected values of the Type I fuel, the results of these analyses are representative of Type II fuel performance.

4. Conclusions. Since the fuel surface heat flux remains low and the maximum fuel temperature does not increase significantly, it is concluded that in the unlikely event of a control rod withdrawal incident from the source range, the reactor core and coolant system would not be adversely affected.

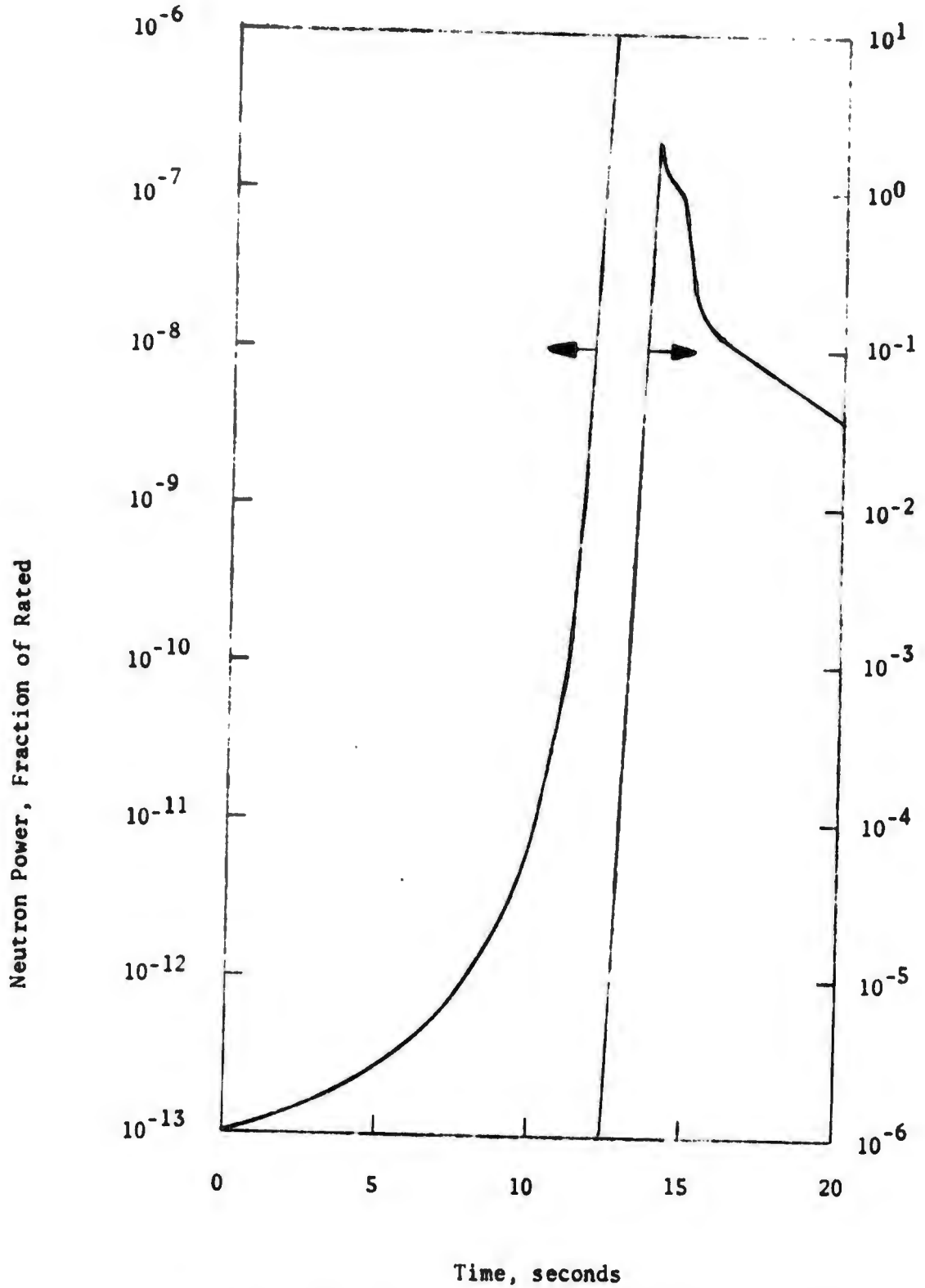

FIGURE 9. SOURCE RANGE ROD WITHDRAWAL TRANSIENT-NEUTRON FLUX VS TIME

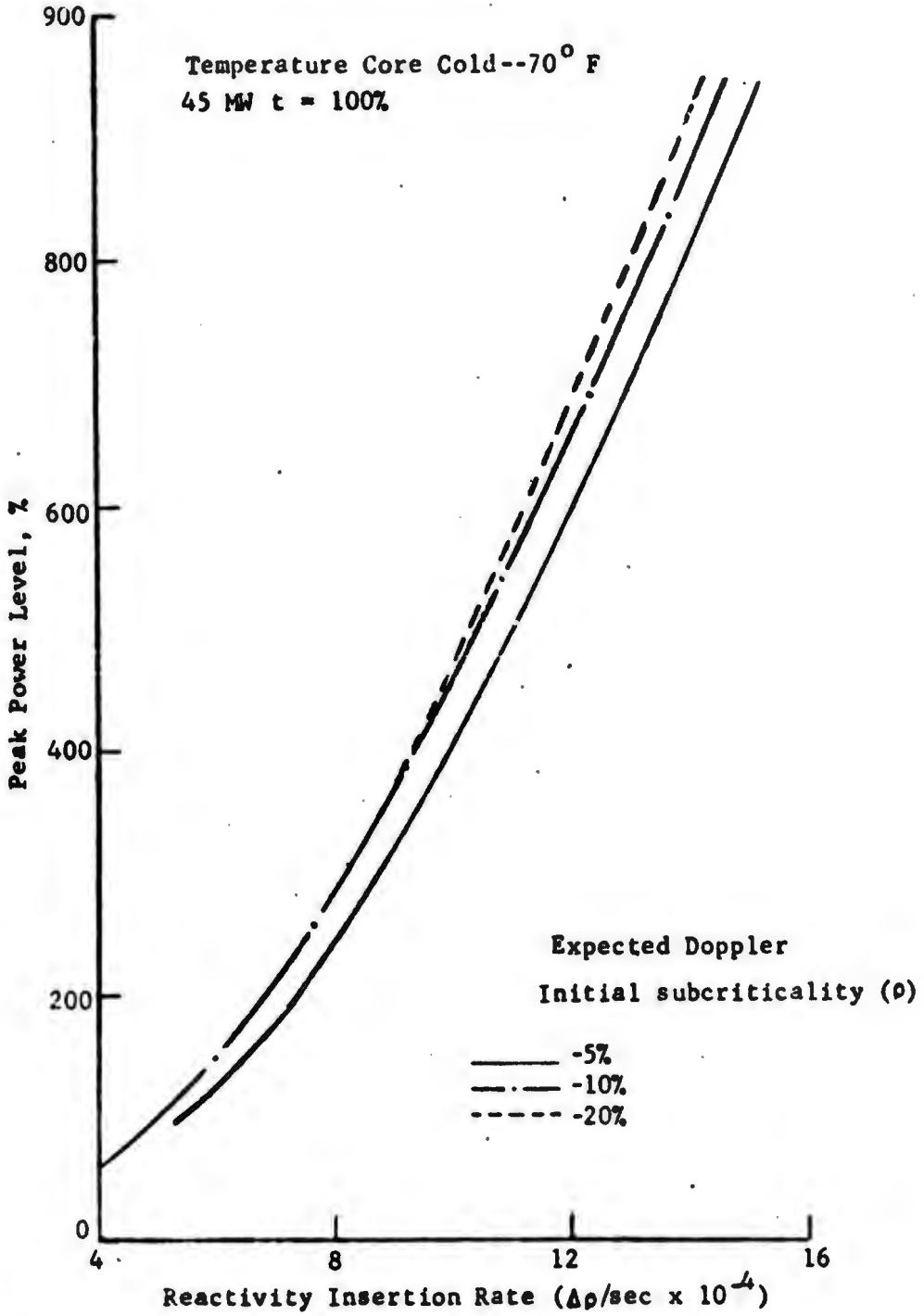

FIGURE 10. EFFECT OF INITIAL SUBCRITICALITY ON PEAK POWER LEVEL DURING ROD WITHDRAWAL ACCIDENT

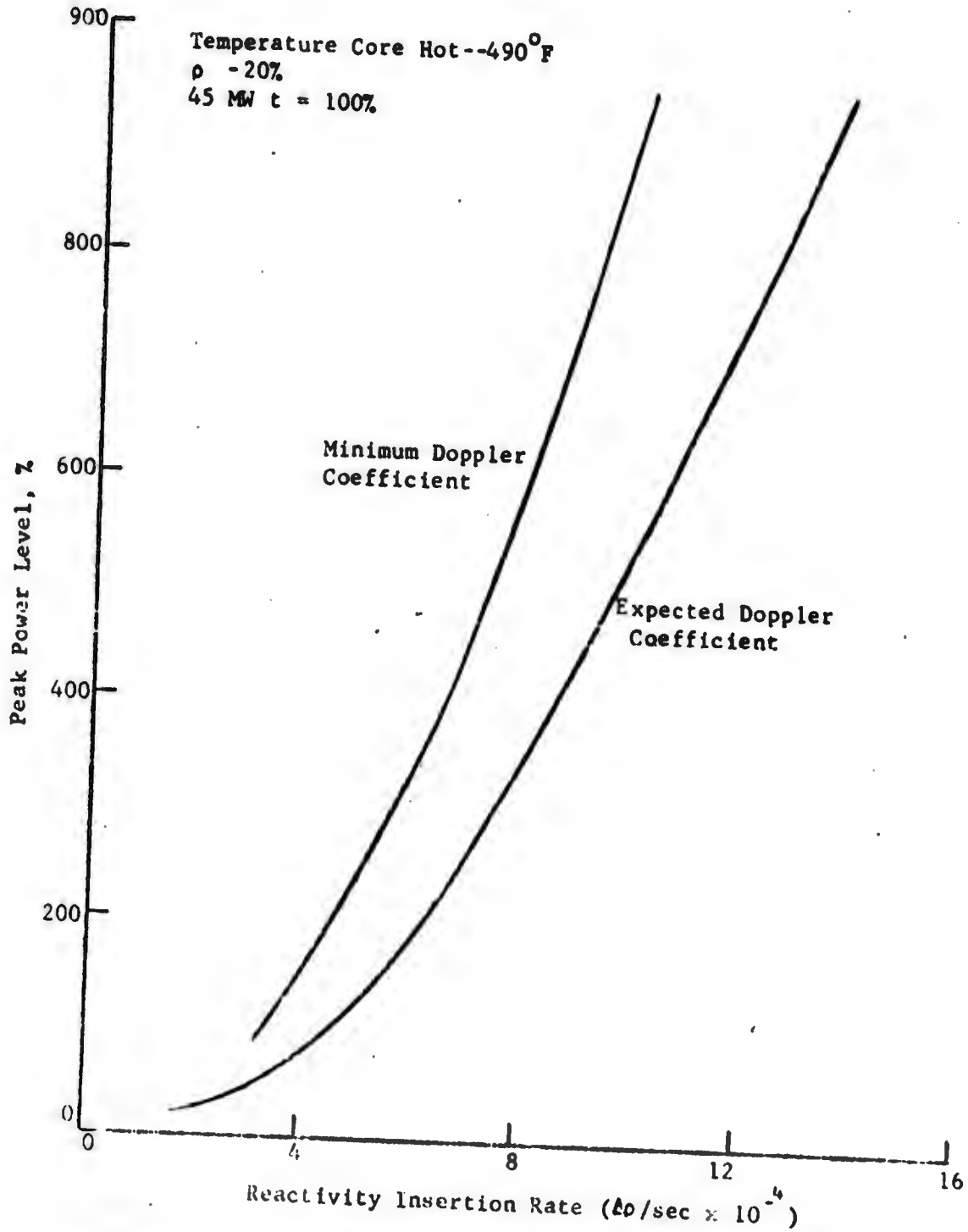

FIGURE 11. DOPPLER REACTIVITY EFFECTS ON POWER LEVELS DURING ROD WITHDRAWAL ACCIDENT

D. Loss of Flow Transient.

1. General. The loss of flow transient (abbreviated LOFT) is defined as either the loss of electric power to or the mechanical failure of one or more reactor coolant pumps. For the MH-1A, it has been shown that the loss of electric power to both reactor pumps represents the most severe transient of this type (Reference 16)[1].

2. Analytical Method. The computer code COBRA was used to calculate the steady-state condition in the hot channel at the desired reactor system parameters (i.e., power, flow, temperature, pressure, etc.). These steady-state conditions were then put into the computer code CHIC-KIN as the starting point for the transient.

To simulate the transient, the reactor system flow rate and power level as functions of time were put into CHIC-KIN. The flow rate versus time curve is shown in Figure 12 and represents the loss of power to both reactor cooling pumps. The core power level versus time curve is shown in Figure 13 and includes a 0.50-second delay time between pump failure and the beginning of control rod motion.

3. Results. The results of the hot-channel analysis at reactor design conditions (111% power) are shown in Figures 14 and 15. These results reflect the effect of fuel densification on power peaking and fuel rod gap conductance.

The hot-channel inlet and exit mass velocities are shown in Figure 14 as functions of time. It will be noticed that the oscillations caused by boiling in the hot channel damp out very rapidly (within 4 seconds). The maximum exit channel quality is less than 16% and decreases with time. Quality at the elevation of minimum DNBR is considerably less. Figure 15 shows the minimum DNBR versus time calculated from the W-3 correlation. The mimimum value is 1.55. Increasing the initial power to 115% results in a mimimum of 1.49.

4. Conclusions. The limiting loss of coolant flow transient initiated from the adverse operating limits does not result in a DNB ratio less than 1.3. This transient assumes a total loss of power to both pumps and maximum delay between pump failure and initial rod motion. Therefore, it is concluded that the reactor can undergo the most severe anticipated loss of flow transient without damage to the core.

---

[1] Schmidt, E. R., et al, "MH-1A Loss of Flow Transient Safety Analysis and Parametric Study", NUS-550, April 1969.

FIGURE 12. FLOW COASTDOWN FOR LOSS OF FLOW TRANSIENT

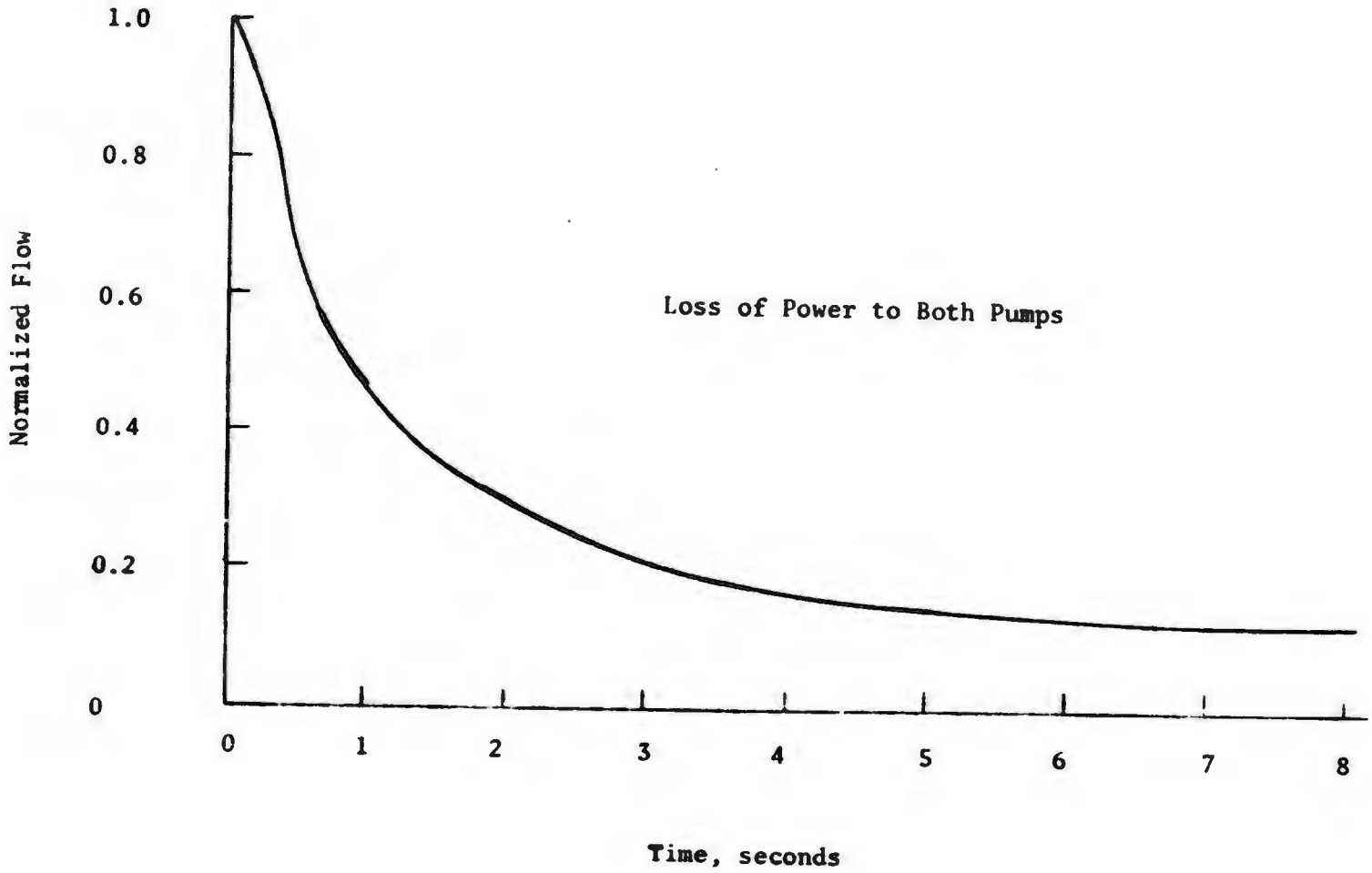

FIGURE 13. REACTOR THERMAL POWER AND NEUTRON FLUX RESPONSE DURING LOSS OF FLOW TRANSIENT

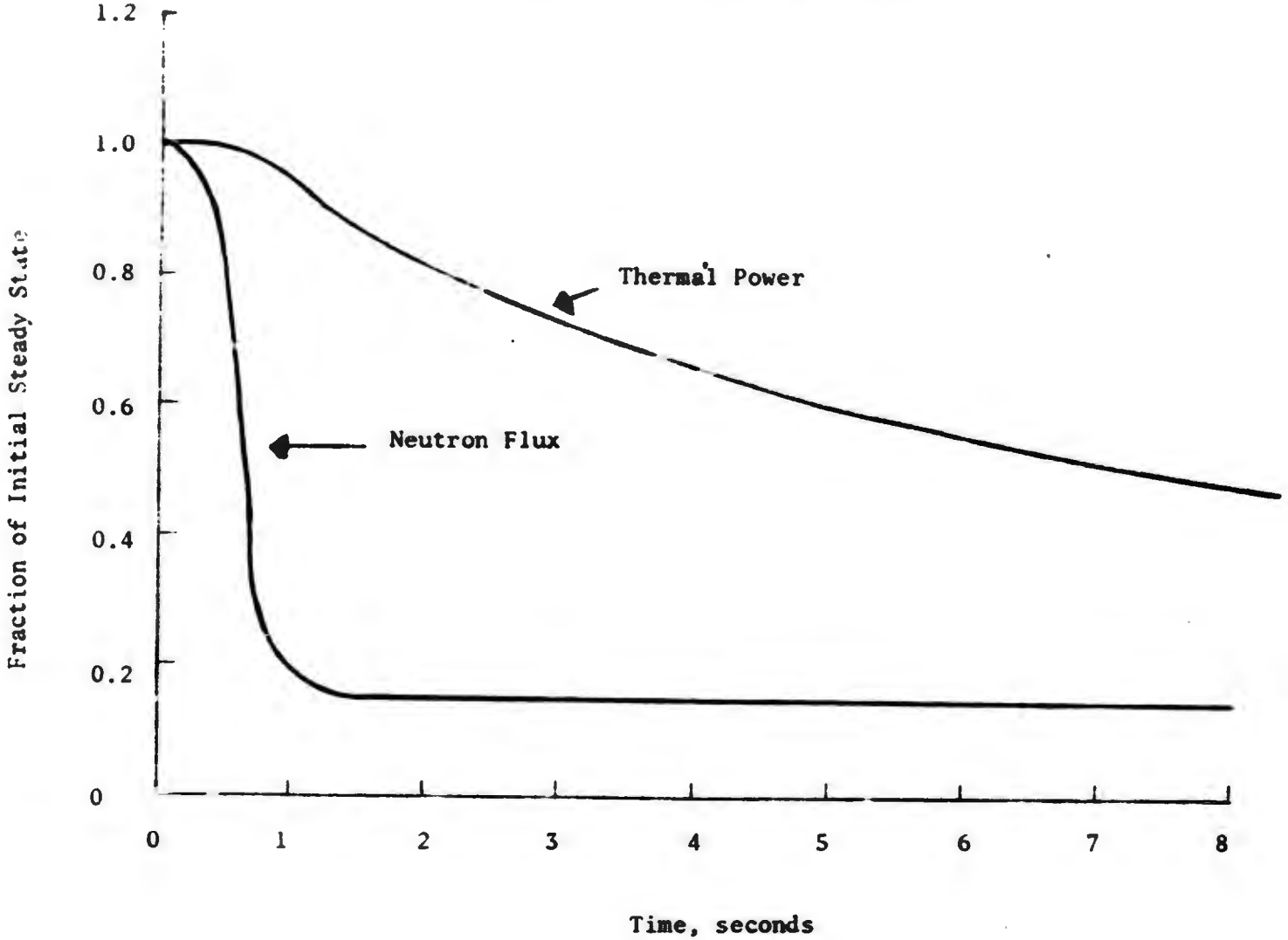

FIGURE 14. HOT CHANNEL MASS VELOCITY VS TIME DURING LOSS OF FLOW TRANSIENT

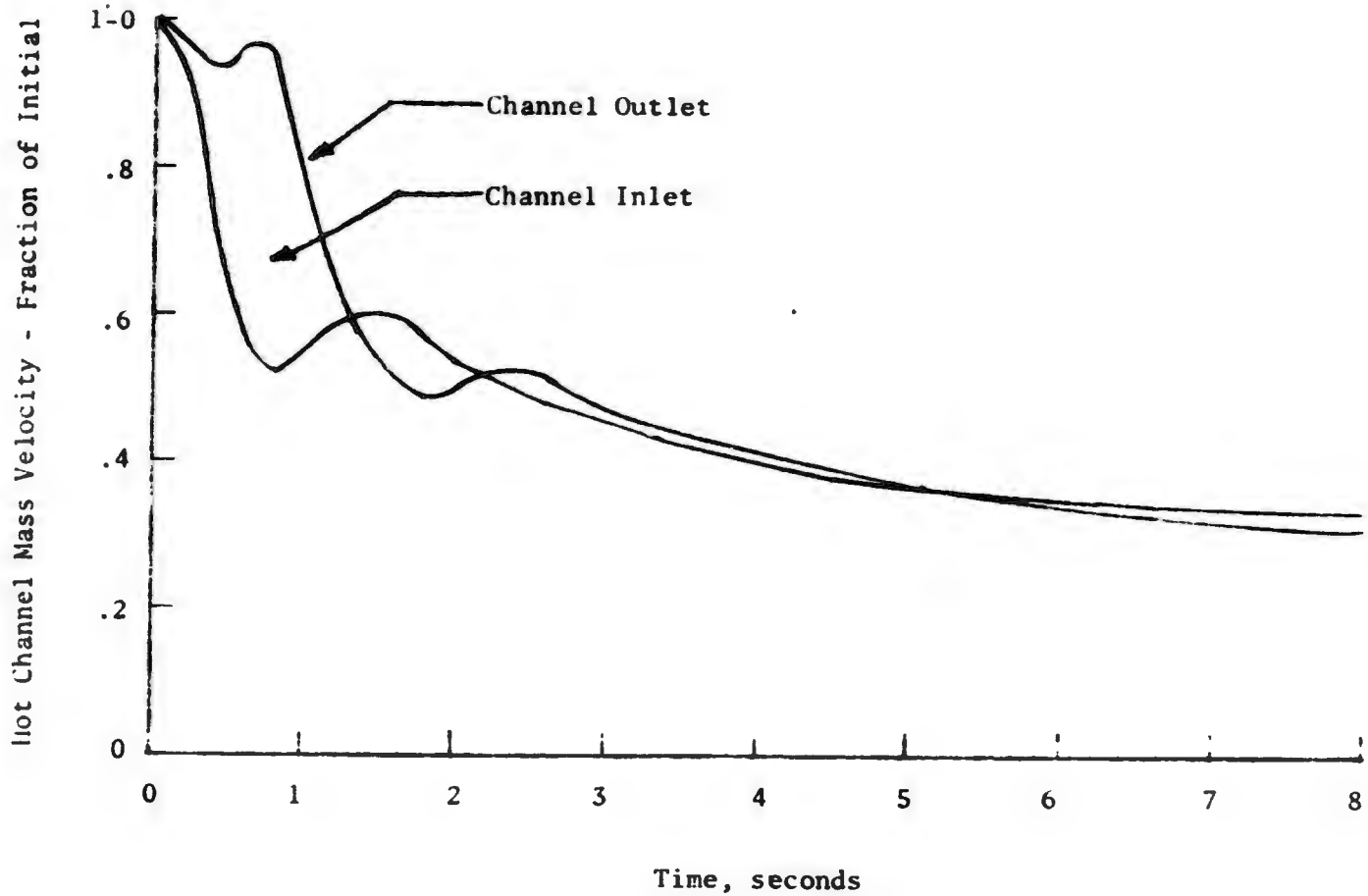

FIGURE 15. MINIMUM DNB RATIO VS TIME AFTER LOSS OF POWER TO BOTH PUMPS

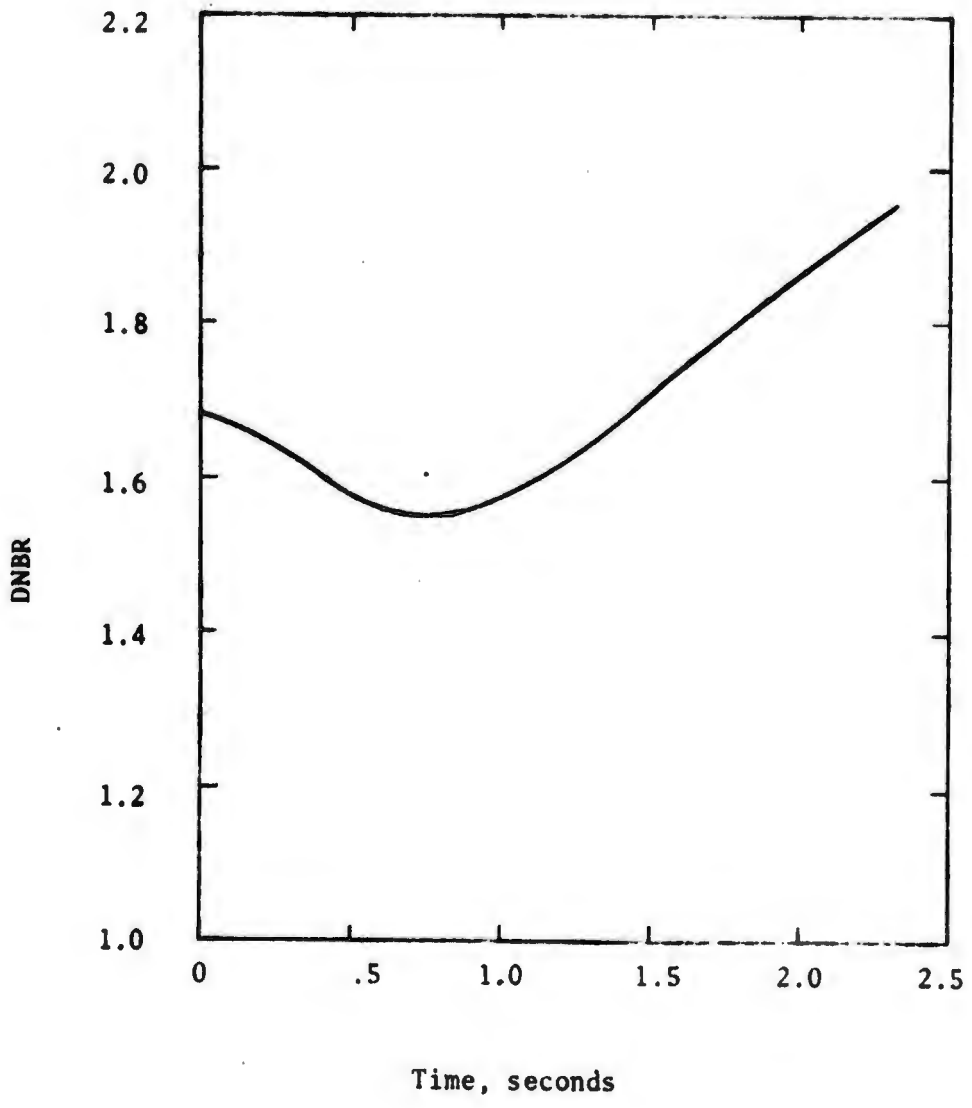

REFERENCES

1. F. E. Muellner, et. al, "Type II Core Design for the MH-1A", NUS-576, Vols. 1 & 2, September 1970.

2. "General Design Criteria for Nuclear Power Plant Construction Permits", Proposed Amendment to 10CFR Part 50, Federal Register Vol. 32, No. 132, July 11, 1967.

3. L. S. Tong, "Prediction of Departure from Nucleate Boiling for an Axially Non-uniform Heat Flux Distribution", J. Nuclear Energy, Vol. 21, (1967).

4. M. F. Lyons, et al, "UO_2 Pellet Thermal Conductivity from Irradiation with Central Melting", GEAP-4624, 1964.

5. S. Y. Ogawa, E. A. Lees, and M. F. Lyons, "Power Reactor High Performance UO Program", GEAP-5591, 1968.

6. D. S. Rowe, "Cross Flow Mixing Between Flow Channels During Boiling, Part 1, COBRA - Computer Program for Coolant Boiling in Rod Arranys", BNWL-371 Part 1, Battelle Northwest, March 1967.

7. "Specification for Fuel Element Assemblies of the MH-1A Type II Core", NYO 10748, New York Operations Office, June 1970.

8. Meyers, C. A., et al., "MH-1A Steady-State and Transient Thermal-Hydralic Design Analysis", ED-6916, USAERG, 25 July 1969.

9. D. S. Rowe and E. W. Angle, "Crossflow Mixing Between Parallel Flow Channels During Boiling", Part II Measurement of Flow and Enthalpy in Two Parallel Channels", BNWL-371 Part 2, Pacific Northwest Laboratory, December 1967.

10. J. A. L. Robertson, " kdt in Fuel Irradiations" CRFD-835, Atomic Energy of Canada Ltd., 1959.

11. Hollis, H. D., et al., "The Theoretical Nuclear Analysis of the MH-1A Core 5", USAENPG, 10 July 1972.

12. Thom, J. R. S., W. M. Walker, T. A. Fallon, and G. F. S. Reising, "Boiling in Subcooled Water During Flow Up Heated Tubes or Annuli", Proc. Instn. Mech. Engs. 1965-66, Vol. 180, Part 3C, 1966.

13. J. S. Christensen, J. J. Allio, A. Biancheria, "Melting Point of Irradiated Uranium Dioxide", WCAP-6065, Westinghouse Atomic Power Division, February 1965.

14. "High Performance UO_2 Program Molten Fuel Rod Operation to High Burnup", Lyons et al, GEAP-5100-2, November 1966.

15. Redfield, J. A. and S. C. Margolis, "TOPS - Fortran Program for the Transient Thermodynamics of Pressurizers", WAPD-TM-515, December 1965.

16. Schmidt, E. R., et al, "MH-1A Loss of Flow Transient Safety Analysis and Parametric Study", NUS-550, April 1969.

17. Redfield, J. A., "CHIC-KIN - A Fortran Program for Intermediate and Fast Transients in a Water Moderated Reactor WAPD-TM-479", January 1965.

18. R. D. Caw, et al, "MH-1A Analog and Controls Analysis", Martin Company, Nuclear Division, 19 Feb 1965.

MH-1A NUCLEAR POWER PLANT

CORE 5

ADDENDUM A TO THE THERMAL HYDRAULIC ANALYSIS

DENSIFICATION EFFECTS IN MH-1A TYPE II FUEL

1 May 1974

DENSIFICATION EFFECTS IN MH-1A TYPE II FUEL

CONTENTS

DENSIFICATION EFFECTS IN MH-1A TYPE II FUEL

1. Introduction and Summary.

This addendum contains an evaluation of fuel densification as it relates to MH-1A Type II fuel design, establishes the power levels for operation during core life, and indicates changes in technical specifications required for such operations.

Fuel densification has been observed to occur in several operating reactors during irradiation (Reference A1)[1]. Densification of UO_2 causes the fuel pellet volume to decrease with a corresponding reduction in fuel pellet radius and length and in fuel column length. Shrinkage of the fuel column can result in axial gaps forming due to incomplete settling of the fuel in the rod and random hangup of the pellets. Potential fuel column gaps can cause local power peaking in adjacent fuel rods due to reduced neutron absorption in the vicinity of the gaps. Also shrinkage of the fuel pellet would increase the linear power density (kw/ft) and reduce the pellet-to-cladding thermal conductance due to increased radial clearance. These conditions result in higher fuel temperatures and hence stored energy and also degrade the heat transfer capability of the fuel during transients.

In Zircaloy-clad fuel, the cladding creeps inward as a function of time, and fuel temperature decreases. Complete collapse of Zircaloy cladding is also possible if sufficiently large axial gaps form and the cladding is not able to resist the external pressure and temperature conditions in the reactor. However the MH-1A stainless steel cladding is essentially free standing, and because of the lower external pressure and greater strength of stainless steel, the MH-1A cladding is not expected to creep-collapse during the life of the fuel. For MH-1A stainless-steel-clad fuel, the initial increase in pellet-clad gap caused by densification is decreased during operation primarily by fuel swelling causing the temperature to decrease with burnup.

The effect of fuel densification on plant operation may be summarized as follows:

1) Increased heat rate and reduced gap conductance result in higher operating temperatures in the fuel, which require a slight reduction in high-power trip setting during the initial portion of core life to maintain adequate margin with respect to the fuel centerline melting criteria.

2) The increase in heat flux due to densification is not of sufficient magnitude to require any changes to the safety limits or accident analyses with respect to Departure from Nucleate Boiling (DNB).

3) The increase in fuel-pellet stored energy may require some reduction in power level during initial core life in order to meet the 2200°F fuel-cladding temperature limit in the event of a loss of coolant accident (LOCA).

---

[1] "Technical Report on Densification of Light Water Reactor Fuels", USAEC Regulatory Staff, November 14, 1972.

The extent of this reduction will depend upon the analyses to be performed in accordance with revised AEC criteria (Reference A2)[1] and upon the final design and installation of the MH-1A Emergency Core Cooling System.

Determination of fuel performance and reactor power capability with densified fuel was made, using the methods and constraints specified by the AEC Regulatory Staff (Reference A1)[2] and utilizing the recommended computer code GAPCON (Reference A3)[3] for computing the fuel-temperature distributions and thermal gap conductance. The results of this analysis are based on the assumption that the MH-1A stainless-steel-clad fuel does not creep-collapse during the life of the fuel and that fuel densification occurs immediately when the reactor is operated at substantial power.

2. Discussion of Fuel Densification.

During the refueling of several commercial reactors it was observed that some Zircaloy-clad fuel rods had developed collapsed or flattened sections. This anomalous behavior was investigated by the AEC Regulatory Staff (Reference A1), which concluded that the observed pellet gaps and collapsed cladding sections were the result of densification of the fuel pellets during operation in the reactor.

In its technical report on fuel densification, the Staff identified the potential effects of densification on fuel performance, proposed methods to evaluate these effects for steady state and transient operation, and required that these phenomena be considered in the design and operation of all light-water reactor fuel. The following specific requirements were stated:

"1. It should be shown that the effects of densification during steady state and transient operation of the reactor do not cause the limits on cladding strain, critical heat flux, and centerline temperatures (previously established in the facility safety evaluation) to be exceeded.

2. The effects of densification should be included in calculating the behavior of the fuel rods during postulated loss-of-coolant accidents. The criteria for evaluating the performance of emergency core cooling systems are presently set forth in the AEC Interim Policy Statement issued in June 1971, which is currently the subject of

---

[1] "Acceptance Criteria for Emergency Core Cooling Systems for Light Water Cooled Power Reactors", DOCKET no., RM-50-1, December 28, 1973.

[2] "Technical Report on Densification of Light Water Reactor Fuels", USAEC Regulatory Staff, November 14, 1972.

[3] G. R. Horn, F. E. Panisko, "GAPCON: A Computer Program to Predict Fuel-to-Cladding Heat Transfer Coefficients in Oxide Fuel Pins", HEDL-TME 72-128, September 1972.

a rulemaking hearing (Docket No. RM 50-1). These criteria or such other requirements that may evolve as a result of the hearing now in progress are to be used.

3. Any operating restrictions necessary to assure that the above conditions are satisfied should be developed and incorporated into the technical specifications for each facility. Additional operating experience and results of experimental programs may indicate that changes in these restrictions or the methods used to derive them are warranted. Flexibility to consider this information has been identified when appropriate....."

An additional requirement placed on fuel with collapsed cladding is not considered applicable because the MH-1A stainless steel cladding is not expected to collapse during the life of the fuel. This is consistent with the conclusions of the AEC regarding performance of stainless-steel-clad fuel with densification (Reference A4)[1]. It should also be noted that additional operating experience and results of current experimental investigations may be the basis for future revision of certain restrictions resulting from densification.

The mechanism of fuel densification is not completely understood at this time, but the currently observed phenomena appear to be related to the initial porosity of the fuel. Typical UO_2 fuel is specified in the range of 90 to 95% of the maximum theoretical density (10.96 gm/cc) with a corresponding void volume or porosity of 5 to 10%. Some porosity in the fuel is desired to offset irradiation-induced swelling of the fuel. Upon densification the fuel density increases to an upper-limit range with a corresponding decrease in pellet volume. The trend is toward increasing fuel shrinkage with decreased initial density.

Densification has been observed to occur in fuel operated at low temperatures and power levels and to occur in relatively short periods of time (2000 hours). It does not appear to be related to thermally induced structural changes known to occur in fuel operated at high powers and temperatures. Until further understanding of fuel densification is obtained, the AEC Regulatory Staff concluded that it should be assumed that all water-reactor fuel densifies immediately when the reactor is operated at substantial power.

The principal effects of fuel densification on fuel performance are:

1) Increased linear heat-generation rate due to axial shrinkage of pellet.

2) Decreased heat transfer capability between pellet and cladding due to radial pellet shrinkage.

---

[1] "Evaluation of Stainless Steel Cladding for Densification and LOCA Conditions: Technical Note 74-1, USAEC Directorate of Licensing, Core Performance Branch, January 1974.

3) Increased stored energy in the fuel.

4) Potential for fuel column gaps causing local power peaking.

An increase in linear heat-generation rate will result if the power produced in the fuel is assumed to remain constant while the fuel shrinks due to densification. This effect is at least partially offset by axial thermal expansion of the fuel. The increased stored energy in the fuel results primarily from the increase in radial clearance between the pellet and cladding causing a decrease in gap conductance. This results in higher fuel temperatures, which affect the power capability and the fuel behavior during a loss of coolant accident (LOCA). A decrease in gap conductance will also degrade the heat-transfer capability of the fuel during transients. Local power peaks can occur, due to reduced neutron absorption, if axial gaps are formed. The magnitude of this effect depends on the size of the gaps formed. In the MH-1A, because of the shorter fuel-column length, only very small gaps could form primarily in the low-power upper region of the core. Also no collapse of the cladding and hence no fuel-cladding interaction is expected during the life of the fuel. This assumption is based on the comparison of MH-1A operating parameters with those of other reactors using stainless-steel-clad fuel (Reference A4) and examination of MH-1A Type I fuel during the past refueling.

3. Fuel Design.

Fuel performance with densification can be affected by fuel design parameters and operating environment. In addition, the fabrication history of the fuel can also be a factor. The fabrication processes for UO_2 pellets and fuel assembly are typical for fuel in the nuclear industry. [2] Consequently no unusual effects are expected for the MH-1A fuel. Design characteristics of the Type II fuel related to fuel performance are briefly summarized below and in Table A1.

The MH-1A Core V is a two-region batch-loaded core designed for a power level of 45 MW_t and expected life of 134 full power weeks. It contains 32 Type II fuel assemblies and 12 cruciform control rods. The 12 inner fuel assemblies contain 92 fuel rods and 12 poison rods, and the 20 outer assemblies contain 96 fuel rods and 8 poison rods. The fuel and poison rods are arranged in an approximate 10 x 10 array to form a fuel assembly. Fuel rods have a nominal active length of 3 feet and contain slightly enriched uranium dioxide pellets. The fuel cladding is 348 stainless steel with a nominal OD of 0.5065 inch and 0.023-inch wall thickness. The UO_2 pellet is 0.4545 inch in diameter and from 0.5 to 1.0 inch long with dished ends. The fuel column is held in place during assembly and shipment by a helical spring in the plenum region of each fuel rod.

The Type II fuel rod is operated at a nominal linear power density of 4.80 kw/ft at rated power.

TABLE A1

SUMMARY OF TYPE II FUEL DESIGN CHARACTERISTICS

Rated Heat Output, MW_t	45	
Core Loading, kg U	2640	
Initial U-235 Enrichment, w/o	7.1	
Core Equivalent Diameter, in	45.2	
Fuel Height, in	36	
	inner	outer
Number of Fuel Assemblies	12	20
Number of Fuel Rods per Assembly	92	96
Poison Rods per Assembly	12	8
Total Number of Fuel Rods in Core	3024	
Average Linear Power, kw/ft	4.80	
Fraction of Power Generated in Fuel	0.966	
Fuel Material	UO_2	
Burnable Poison	B_4C in Zr	
Clad Material	348 SS	
Cold Dimension		
Clad OD, in	.5065	
Clad Thickness, in	.023	
Pellet OD, in	.4545	
Diametral gap, in	.006	
Pellet Density, % Theoretical		
Nominal as-fabricated	93.4	
2σ variation	$\pm$0.6	
Fill Gas Composition		
Pressure, psia	14.7	
% Helium by volume	95.0	
Maximum Clad OD Temperature °F		
1500 psia	612	
1400 psia	603	

4. Analytical Methods.

a. GAPCON.

The analysis of the densification effects in the MH-1A fuel pins is performed using the computer code GAPCON (Reference A3). This program calculates the steady-state fuel-temperature distribution and pellet-to-cladding thermal conductance considering the effects of

- fuel and cladding thermal expansion
- fill-gas composition and conductivity
- sorbed-gas release
- fission-gas generation and release
- fuel thermal restructuring
- fission-product induced swelling
- gap closure and contact conductance

Variation of these effects with time and with linear heat rating can be computed for various combinations of fuel parameters and operating conditions. Input to this program includes fuel and clad dimensions, fuel composition, density, UO_2 thermal conductivity, power distribution, and fuel-pin operating conditions.

Comparisons of GAPCON calculations with experimental data (Reference A5)[1] shows good agreement for short irradiations. However GAPCON as presently written assumes constant operating levels and conditions and does not follow the actual fuel-pin operating history. Also the only mechanisms for fuel to cladding gap closure treated by the program are thermal expansion and fission-product induced swelling. Experimental data indicate that a significant mechanism for gap closure is relocation of the fuel due to cracking of the pellets and movement of the fuel into the gap (Reference A11). In this sense GAPCON predicts conservatively high fuel temperatures and low gap conductance for other than short-term irradiation.

In performing calculations with GAPCON, the following assumptions were made:

1) Fuel swelling was computed by the relations of Geithoff, et al (Reference A3). No credit was taken for increased rate of gap closure due to fuel cracking.

---

[1] C. R. Hann, "Fuel Rod Gap Conductance and UO_2 Thermal Conductivity", Study for AEC Directorate of Licensing, July 1972.

[2] O. C. Ditmore, et al, "Densification Considerations in Boiling Water Reactor Fuel Design and Performance", NEDM-10735, December 1972.

2) The flux depression in the fuel pellet was obtained from Reference A6[1] based on enrichment and fuel-rod diameter.

3) The fission-gas release rate was obtained from UO_2 irradiation data of Hoffman and Coplan (Reference A7)[2], which correlates the fractional release to the fuel volumetric average temperature. The fission-gas release rate at the hot spot was divided by the time-averaged axial peaking factor (1.5) to obtain the average rod-release rate.

4) The UO_2 thermal conductivity as a function of temperature was based on the data of Lyons (Reference A8, A9)[3] with a conductivity integral of 93 w/cm.

5) Densification was assumed to occur at the beginning of core life and to result in increased fuel density and pellet-to-cladding gap.

6) The fuel-pin power and operating conditions were assumed constant during burnup calculations. The actual power densities would decrease with fuel burnup.

7) No gap closure due to creep-down of the cladding onto the fuel was permitted.

These assumptions are consistent with those used by the AEC Regulatory Staff in their evaluation of Maine Yankee fuel densification (Reference A10)[4] using the GAPCON computer program.

Calculations were performed for the MH-1A fuel pin to evaluate the radial gap conductance for densified fuel as a function of linear heat rate, burnup, pellet density, cold gap dimensions, and UO_2 conductivity. Results of these calculations indicated that changes in gap conductance due to densification were primarily the result of changes in pellet-to-cladding clearance. Figure A1 shows the effect of cold diametral gap on the predicted gap conductance for various linear heat rates. These calculations were performed in the beginning of core life. The gap conductance changes during burnup, as a result of fission-gas generation and release and irradiation-induced fuel swelling. The net result is an initial decrease in gap conductance due to

---

1 J. A. L. Robertson, "$\int$kdt in Fuel Irradiations" CRFD-835, Atomic Energy of Canada Ltd., 1959.

2 J. P. Hoffman and D. H. Coplin, "The Release of Fission Gases from Uranium Dioxide Pellet Fuel Operated at High Temperatures" GEAP-4596, September 1964.

3 M. F. Lyons, et al, "UO_2 Pellet Thermal Conductivity from Irradiation with Central Melting", GEAP-4624, 1964.

3 S. Y. Ogawa, E. A. Lees, and M. F. Lyons, "Power Reactor High Performance UO_2 Program" GEAP-5591, 1968.

4 "Addendum to Safety Evaluation - Fuel Densification and its Effects", Maine Yankee Nuclear Plant, DOCKET 50309-105, USAEC Directorate of Licensing, March 1973.

FIGURE A1. GAP CONDUCTANCE AS FUNCTION OF COLD DIAMETRAL GAP FOR MH-1A FUEL PIN

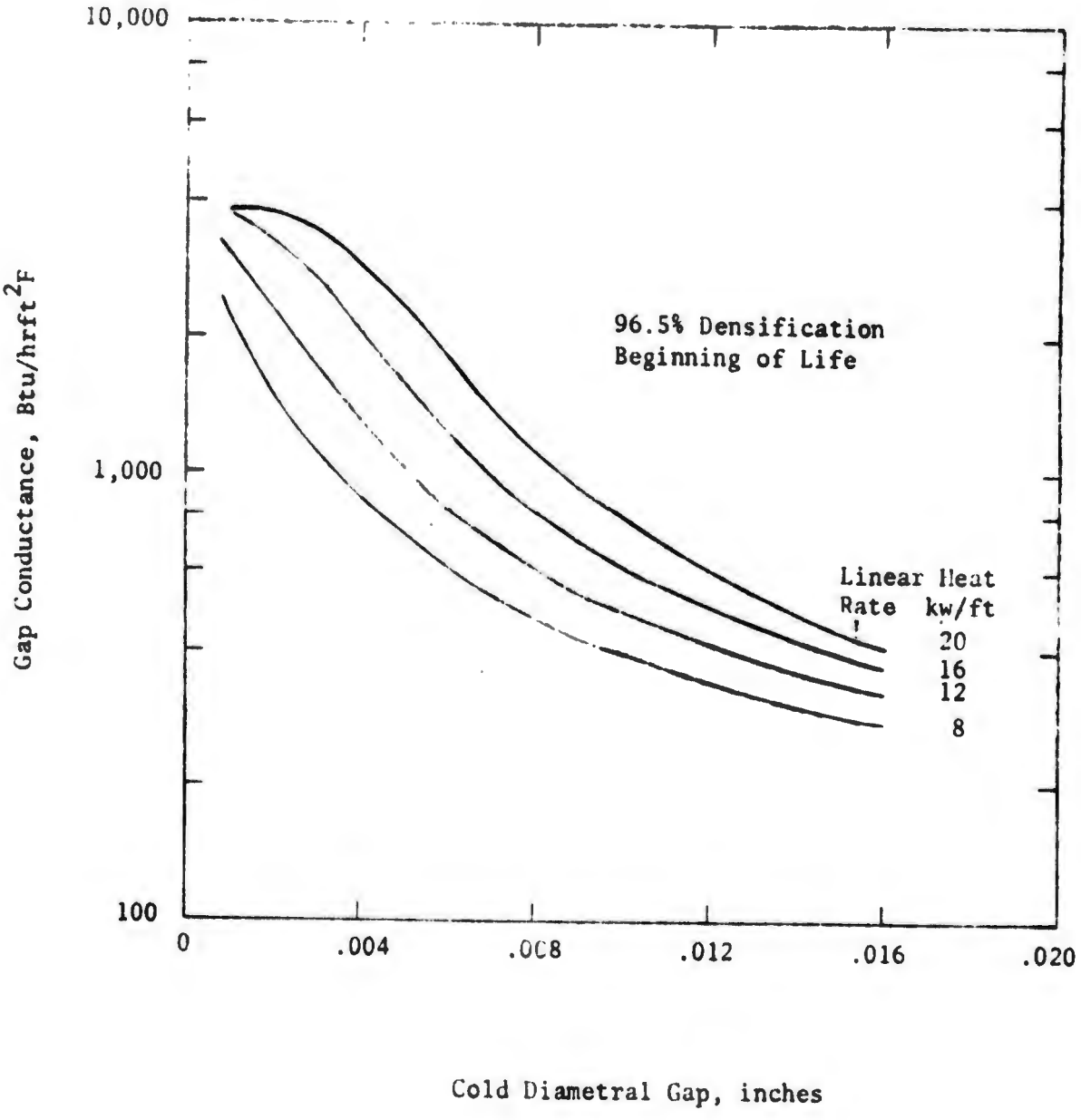

release of fission gases to the gap and subsequent increase as swelling reduces the gap width. The additional effect of pellet cracking and relocation as mentioned previously would increase the rate at which the gap closes and significantly reduce fuel temperatures early in core life. However, since sufficient data are not available at present to quantify this effect, it has been conservatively neglected in the analyses.

b. Densification Penalties.

Local power can be increased due to densification by the formation of axial gaps in the fuel column and by a reduction in fuel length. These effects are analyzed in accordance with the methods outlined by the AEC in their technical report (Reference A1). Local power peaking due to gap formation is determined on the basis of the following conservative assumptions:

1) All fuel rods densify to the maximum extent at the beginning of core life.

2) Axial gaps are formed randomly due to densification and incomplete settling of the fuel pellets.

3) The maximum gap size varies directly with height from the bottom of the fuel according to

$$\Delta L = \frac{(.965-\rho)\ L}{2}$$

where ΔL is the maximum gap size, L is the axial height in the fuel column and ρ is the as-fabricated mean density.

4) The most adverse combination of gap size and power peaking are assumed to occur in the limiting fuel rod. Statistical evaluation of the variation and frequency of gap sizes throughout the core would result in a lower value of peaking due to densification.

The mean fuel density for the most limiting core region is 93.4% theoretical density(1). The maximum reduction in fuel-column height is therefore 1.6% (0.56 inches) at the top of the core. However, axial thermal expansion results in an increase in fuel-column length of 0.9% based on an average pellet temperature of 1800°F at the outer edge of the pellet dish and a UO_2 thermal expansion coefficient of 5.0×10^{-6}/°F. Therefore the net decrease in pellet stack height is 0.7% (0.25") at the top of the core. Considering that the limiting peak power occurs at elevations less than 20" through most of core life, the maximum gap size affecting power peaking is 0.14 inch. On the basis of reported results (Reference A1) the maximum effect of this gap size on local power is estimated as 1.2%. Statistically the probability that this gap will form on the limiting fuel rod is small.

---

(1) Based on as-fabricated fuel density of centrally loaded assemblies KM 57. KM 60, KM 62, KM65.

The effect of fuel densification on linear heat rate is evaluated in accordance with AEC assumptions for decrease in pellet length.

$$\Delta L = \frac{(.965 - \rho + 2\sigma)L}{2}$$

where: ΔL = decrease in pellet length
L = length of pellet
ρ = initial mean density, fraction of theoretical
σ = standard deviation of measured density

The local increase in heat-generation rate is based on the as-fabricated mean pellet density and 2σ variation of $93.4 \pm 0.6\%$ theoretical resulting in a length decrease of 1.9% due to densification. Axial thermal expansion under operating conditions is 1.3% based on a pellet temperature of 2200°F at the outer edge of the pellet dish and the UO_2 thermal expansion coefficient of 6×10^{-6}/°F at the location of peak power. This results in a net increase in heat-generation rate (kw/ft) of 0.6%. Use of this factor conservatively neglects the decrease in fissionable U-235, which would result from the assumed lower-than-average initial pellet density.

The net effect of densification on power peaking is summarized below:

Power peak due to axial gaps	1.012
Decrease in pellet length	1.019
Thermal expansion	.987
Total increase due to densification	1.018

c. Fuel-Temperature Evaluation.

The effects of fuel densification result in an increase in fuel temperatures due to increased power peaking and reduced gap conductance. The maximum increase in pellet cladding radial gap is computed assuming that the fuel densifies at the beginning of core life and that the fuel radius decreases in accordance with

$$\Delta r = \frac{(.965 - \rho + 2\sigma)r}{3}$$

where Δr is the decrease in pellet radius, r is the nominal pellet radius and the mean density and 2σ variation are based on the as-fabricated pellet densities. The resulting cold diametral gap is 0.0116 inch which is decreased at operating power levels due to differential thermal expansion of the fuel and clad.

The pellet temperature distribution and gap conductance are computed using the computer program GAPCON as discussed in Section 4a. Figure A2 shows the results of the calculation of the fuel centerline temperature of the hot pellet as a function of linear heat rate and fuel burnup. These

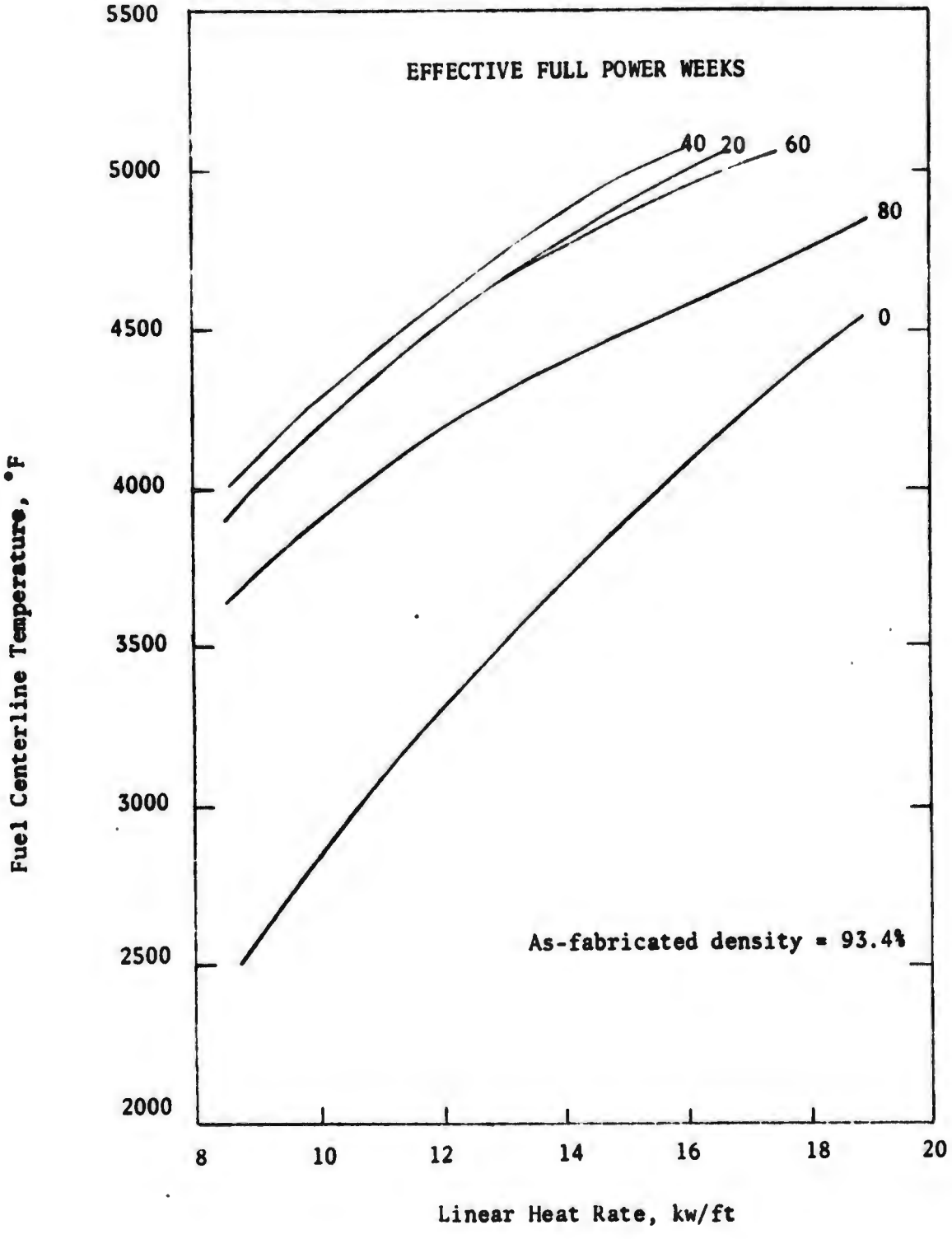

FIGURE A2. FUEL CENTERLINE TEMPERATURE VS LINEAR HEAT RATE FOR DENSIFIED FUEL

calculations utilize the as-fabricated density as discussed previously and assume that densification occurs immediately at beginning of core life. No creep-down of the cladding is assumed, but the radial gap conductance is improved during operation by irradiation-induced fuel swelling and thermal expansion. As mentioned previously no credit is taken for gap closure from the observed effects of fuel relocation due to pellet cracking. It is expected that this effect would significantly decrease the fuel temperatures early in core life and would be essentially irreversible.

In evaluating transients the increased fuel temperatures and reduced gap conductance are factored into the analysis. Behavior of the fuel during loss of coolant accident (LOCA) conditions is affected by fuel average temperature or stored energy. Since LOCA calculations are sensitive to fuel-assembly average stored energy, the pellet diameter and gap size are calculated using the mean pellet density for the limiting fuel assemblies. Figure A3 shows the results of the calculation of fuel-pellet average temperature as a function of linear heat rate and fuel burnup. These calculations assume that the fuel densifies immediately at the beginning of core life. The initial increase in fuel temperature is due to the generation and release of fission gas which degrades the gap thermal conductance. The subsequent decrease in fuel temperature results from the effects of irradiation-induced fuel swelling. Temperatures continue to decrease to the end of core life.

d. Departure from Nucleate Boiling (DNB) Evaluation.

The increase in local power due to densification could result in a slight decrease in DNB heat flux ratio in the core. In evaluating DNB it is conservatively assumed that power peaking due to densification occurs at the location of minimum DNB ratio. This effect is small and has no significant effect on normal operation.

During transients the decreased heat-transfer capability due to densification could decrease the minimum DNB ratio for certain transients (such as the loss of flow transient). In those cases the effect of radial gap conductance is factored into the transient analyses.

5. Effect on Normal Operation and Transients.

As noted previously fuel densification can result in increased local power density, increased stored energy in the fuel, and reduced pellet-cladding gap conductance. These effects result in changes in normal steady-state and transient operation as well as affecting fuel performance under loss-of-coolant accident conditions. This section examines the effect of densification on plant operations and establishes the operating restrictions necessary to assure adequate margin of safety with respect to fuel design limits.

a. Overpower Limits.

The basis for evaluating the overpower limits is the criterion of no fuel centerline melting during normal operation or anticipated transient.

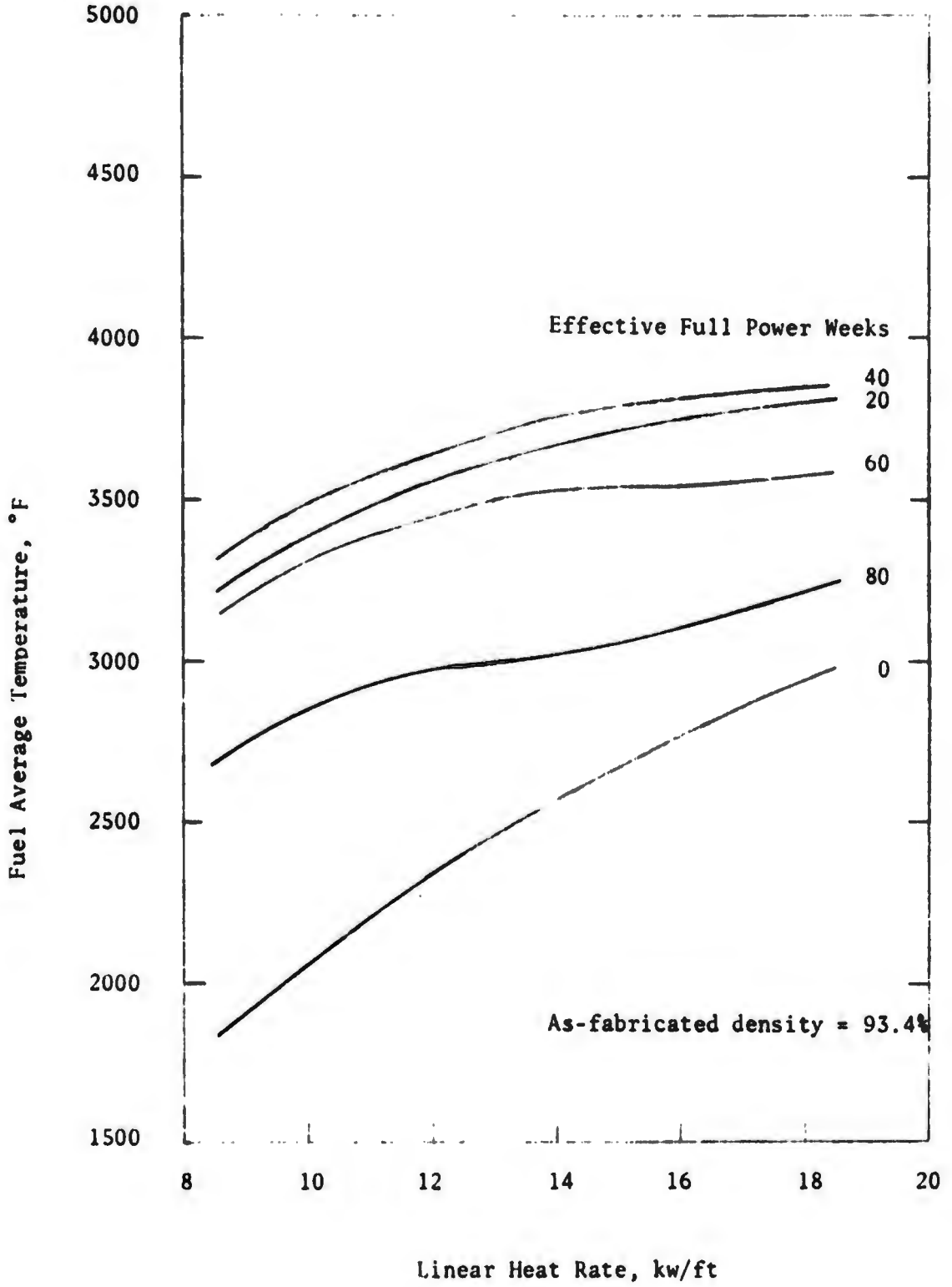

FIGURE A3. FUEL AVERAGE TEMPERATURE VS LINEAR HEAT RATE FOR DENSIFIED FUEL

To establish the power capability of the core with densified fuel, the local linear power necessary to cause fuel melting as a function of burnup is compared with the peak rod power at rated conditions. Adequate margin is assured by appropriate setting of the high-power level trip.

The peak rod power at rated conditions without densification is shown in Table 2 as a function of fuel burnup. This includes a 10% uncertainty in power distribution and a 3% uncertainty due to manufacturing tolerances. Since equilibrium Xenon operating conditions are assumed, a restriction has been placed on the rate at which a return to power can be accomplished after an extended shutdown. The purpose of the specification is to assure favorable Xenon distribution during operation at or near full power. It does not limit normal operational transients nor does it limit the rate at which power level may be decreased.

The nominal power-level trip is 110% of rated power. Any reduction in set point is computed from

$$\text{Reduction in power level trip} = \frac{\text{Rod-power limit (kw/ft)}}{\text{Rod-power at 45 MW}_t \text{ (kw/ft) } 1.18\ 1.018}$$

where 1.18 is the minimum overpower margin that includes allowance for setpoint error and transient overshoot, and the 1.018 factor is the densification penalty due to power peaking. The rod-power limit for densified fuel is based on UO_2 melting temperature (Reference 12)[1] of 5080°F unirradiated, decreasing by 58° per 10,000 MWD/MT of fuel burnup. Figure A4 shows the rod-power limit to meet the fuel centerline criterion as a function of core burnup. The power-level setpoint reduction necessary to assure that this limit is not exceeded is given in Section 6, Revision to Technical Specifications. The initial decrease in limiting rod power is due to the generation and release of fission gases which reduce the pellet-cladding gap conductance, while the subsequent increase is due to irradiation-induced fuel swelling which closes the gap and reduces fuel temperature.

b. Transient Limits.

In evaluating transients the effects of densification have been included in the analyses. In most cases the results of the transients are not changed significantly, and adequate margins are maintained between transient limits and core safety limits. The effects of densification on DNB and core void fraction are less severe than the effects on fuel temperature and are in general compensated for by the reduced permissible rod power (kw/ft).

Analyses show that for limiting transients involving increases in power level, the core is adequately protected by the high-power-level trip.

---

[1] J. A. Christensen, et al, "Melting Point of Irradiated Uranium Dioxide", WCAP-6065, February 1965.

TABLE A2

PEAK THERMAL POWER AT RATED CONDITIONS vs BURNUP

Effective Full-Power Weeks	Peak Burnup MWD/MTU	Peak Rod Power kw/ft
0	0	16.0 (1)
20	7,000	14.6
40	14,000	14.3
60	21,000	14.2
80	29,000	13.5
134	44,000	14.0

(1) Beginning of life equilibrium Xenon. Peak rod power is reduced to 14.9 kw/ft after approximately two full-power weeks.

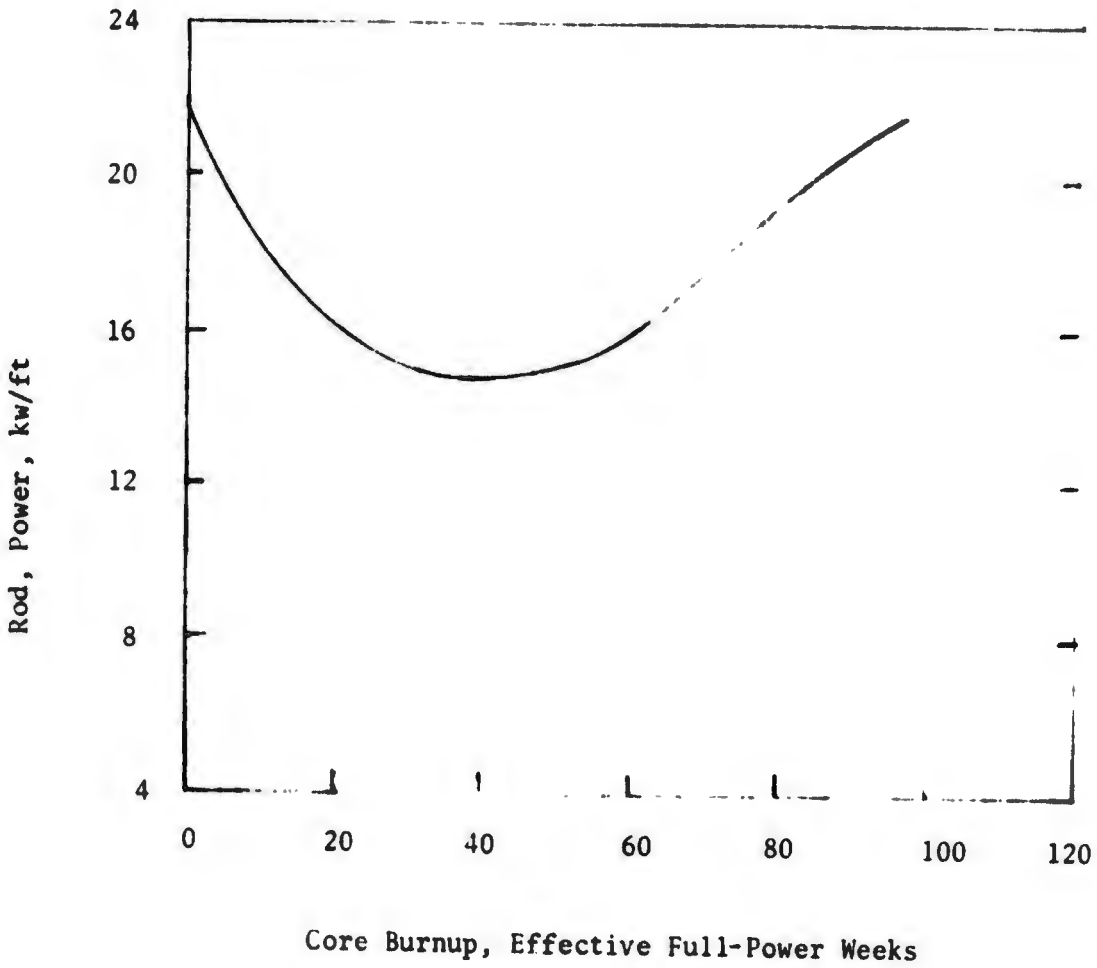

FIGURE A4. ROD POWER LIMIT VERSUS CORE BURNUP

These include rod withdrawal in the power range and during source-level startup and steam-line rupture transients. For a loss-of-coolant-flow transient, the effect of higher initial fuel temperatures and reduced gap conductance can result in a lower DNB ratio. Analyses indicate that the minimum DNB ratio considering densification is reduced slightly but that sufficient margin is maintained to the design limit of 1.3. Normal operation and operational transients such as load changes are well within the core safety limits and no significant effect on fuel performance due to densification is anticipated.

c. Loss-of-Coolant Accident Limits.

The increased stored energy in the fuel due to densification can result in changes in peak cladding temperatures during a postulated Loss-of-Coolant Accident. Analyses will be performed to develop a limit on maximum stored energy (fuel average temperatue) as a function of linear heat rate that assures a peak cladding temperature of less than 2200°F. This limit will be compared with fuel average temperatures versus burnup for densified fuel (Figure A3) to establish permissible operating power levels as a function of core burnup. The analyses will be consistant with the current AEC criteria on ECCS (Reference A2) and will be based on the final design of the MH-1A ECCS.

6. Revision to Technical Specifications.

Revisions have been made to the technical specifications to reflect the effects of fuel densification. These changes relate to the safety limits and safety system setting on high power level and to the rate of increase in power during operations.

The changes made to the technical specifications are presented below. The paragraph numbering sequence used corresponds to the existing within the technical specifications. Unless otherwise noted, sections omitted remain unchanged.

1. SAFETY LIMITS - REACTOR CORE

c. Specification: (1) The combination of thermal power, reactor outlet temperature and primary system pressure shall not exceed the limits shown in Figure 2. These limits are considered to be exceeded if the point defined by the combination of coolant temperature and power level is at any time to the right of the appropriate system pressure line.

(2) The reactor thermal power shall not exceed the limits shown in section 3c (1) (b).

d. Basis: The effects of fuel densification have been included in the evaluation of DNB and of fuel temperature during core burnup. Fuel densification results in increased local power density

and reduced pellet-to-cladding thermal conductance, which increases fuel temperature and heat flux during operation. These effects have been considered in the development of core safety limits. In order to assure that the fuel center temperature does not reach the UO_2 melting temperature, an additional limit has been placed on the reactor thermal power level. This limit considers the variation of fuel temperature and power peaking with burnup, and in conjunction with the power level trip setting, assures that fuel design limits are not exceeded.

NOTE: Replaces Section 1c and paragraph 4 of Basis.

3. LIMITING SAFETY SYSTEM SETTINGS

c. Specification: (1) High Reactor Power - The limiting setpoint shall be the lower of

(a) ≤ 110% of rated thermal power

(b) ≤ value shown below at intervals subsequent to the beginning of life as described in the basis of this specification

Fuel Burnup, Effective Full-Power Weeks	Limiting Safety System Setting, % 45 MW	Safety Limit, % 45 MW
0 to 5	≤ 110	118
5 to 10	105	117
10 to 20	100	110
20 to 30	96	105
30 to 50	94	103
50 to 60	96	105
60 to 70	102	112
> 70	110	118

d. Basis: The specified safety system settings with allowance for error provide assurance that the combination of power, temperature, pressure and flow will not exceed the core safety limits as stated herein. The criterion for high-power-level setpoint is that core power be prevented from reaching a value at which fuel centerline melting would occur. For a given power density, fuel temperatures first increase due to fission-gas buildup and then decrease due to irradiation-induced swelling. Therefore core power limit and limiting safety system settings change accordingly.

Changes in power-level trip setting shall be done in a series of discrete steps at intervals determined by review and approval of Plant Safety Committee following the limits shown in Section 3 c (1).

NOTE: Replaces Section 3 c (1) and first paragraph of Basis.

SECTION IV. LIMITING CONDITIONS FOR OPERATION

11. **RATE OF POWER INCREASE**

a. **Applicability:** This specification applies to the rate at which power may be increased for a core burnup of less than 70 effective full-power weeks.

b. **Objective:** The purpose of this specification is to prevent adverse power distribution due to Xenon effects.

c. **Specification:** Should a power level of less than 50% of rated power be maintained for more than 10 hours, the rate of increase between 50% and 100% power shall be limited to 5% per hour.

d. **Basis:** This specification assures that power density will remain within design values by providing sufficient time for power redistribution due to Xenon buildup.

REFERENCES

A1. "Technical Report on Densification of Light Water Reactor Fuels", USAEC Regulatory Staff, November 14, 1972.

A2. "Acceptance Criteria for Emergency Core Cooling Systems for Light Water Cooled Power Reactors", DOCKET No. RM-50-1, December 28, 1973.

A3. G. R. Horn, F. E. Panisko, "GAPCON: A Computer Program to Predict Fuel-to-Cladding Heat Transfer Coefficients in Oxide Fuel Pins", HEDL-TME 72-128, September 1972.

A4. "Evaluation of Stainless Steel Cladding for Densification and LOCA Conditions", Technical Note 74-1, USAEC Directorate of Licensing, Core Performance Branch, January 1974.

A5. C. R. Hann, "Fuel Rod Gap Conductance and UO_2 Thermal Conductivity", Study for AEC Directorate of Licensing, July 1972.

A6. J. A. L. Robertson, "$\int$kdt in Fuel Irradiations", CRFD-835, Atomic Energy of Canada Ltd., 1959.

A7. J. P. Hoffman and D. H. Coplin, "The Release of Fission Gases from Uranium Dioxide Pellet Fuel Operated at High Temperatures", GEAP-4596, September 1964.

A8. M. F. Lyons, et al, "UO_2 Pellet Thermal Conductivity from Irradiation with Central Melting", GEAP-4624, 1964.

A9. S. Y. Ogawa, E. A. Lees, and M. F. Lyons, "Power Reactor High Performance UO_2 Program", GEAP-5591, 1968.

A10. "Addendum to Safety Evaluation - Fuel Densification and its Effects", Maine Yankee Nuclear Plant, DOCKET 50309-105, USAEC Directorate of Licensing, March 1973.

A11. O. C. Ditmore, et al, "Densification Considerations in Boiling Water Reactor Fuel Design and Performance", NEDM-10735, December 1972.

A12. J. A. Christensen, et al, "Melting Point of Irradiated Uranium Dioxide", WCAP-6065, February 1965.